Assessment of errors in SIMS zircon U–Pb geochronology using a natural zircon standard and NIST SRM 610 glass

Richard A. Stern[a,*], Yuri Amelin[b]

[a] *J.C. Roddick Ion Microprobe Laboratory, Geological Survey of Canada, Natural Resources Canada, Ottawa, ON, Canada K1A 0E8*
[b] *Royal Ontario Museum, 100 Queen's Park, Toronto, ON, Canada M5S 2C6*

Abstract

Analytical errors calculated for individual spot $^{206}Pb/^{238}U$ measurements of zircon analyzed using high mass resolution secondary ion mass spectrometry (HR-SIMS, e.g., SHRIMP II) were assessed using natural zircon (z6266) and synthetic glass standards (NIST SRM 610). Evidence for U/Pb homogeneity of these materials includes new thermal ionization mass spectrometry (TIMS) U–Pb analyses of 22 fragments of z6266 zircon from two laboratories, which are identical within error and yield a weighted mean $^{206}Pb/^{238}U$ age of 559.0 ± 0.2 Ma. TIMS U–Pb analyses of the SRM 610 yielded homogeneous $^{206}Pb/^{238}U = 0.2566$.

Errors in HR-SIMS $^{206}Pb/^{238}U$ measurements are distinguished in increasing hierarchy as within-spot, within-session (internal), and external. Replicate SHRIMP measurements of $^{208}Pb^+/^{206}Pb^+$ and $^{248}[ThO]^+/^{254}[UO]^+$ in SRM 610 demonstrate that within-spot analytical errors are sufficient (i.e., MSWD's ~ 1) to account for the dispersion of data. In contrast, it was not possible with SRM 610 to reproduce the $^{206}Pb^+/^{238}U[O_{x=0,1,2}]^+$ ratios from spot-to-spot within the limits of the within-spot errors, after correcting the data for obvious systematic variations in the discrimination of the Pb and U isotopes. Identical findings were made following replicate $^{206}Pb^+/^{238}U[O_x]^+$ analyses of z6266 zircon. That is, for both glass and zircon standards, there remained on average about $\pm 1\%$ (1σ) unaccounted variation per $^{206}Pb^+/^{238}U[O_x]^+$ analysis (i.e., MSWDs$\gg$1). Thus, unlike for $^{248}[ThO]^+/^{254}[UO]^+$, the within-session errors in $^{206}Pb^+/^{238}U[O_x]^+$ were necessarily higher than the within-spot errors.

In contrast to $^{208}Pb^+/^{206}Pb^+$ and $^{248}[ThO]^+/^{254}[UO]^+$, the $^{206}Pb^+/^{238}U[O_x]^+$ ratios in glass and zircon are significantly fractionated relative to accepted values, and it seems probable that this difference underlies the larger within-session errors for $^{206}Pb^+/^{238}U[O_x]^+$. The usual methods (e.g., using $^{254}[UO]^+/^{238}U^+$) to correct for the inherent discrimination are imperfect and sensitive to small differences in analytical conditions between spots. Matrix variations are ruled out, leaving the precise cause(s) of the additional variation in $^{206}Pb^+/^{238}U[O_x]^+$ currently undetermined, and a hindrance to decreasing the uncertainties in spot $^{206}Pb/^{238}U$ measurements. The minimum within-session error for an individual $^{206}Pb/^{238}U$ measurement is the standard deviation (dispersion) of the discrimination-corrected $^{206}Pb^+/^{238}U[O_x]^+$ values for a homogeneous reference material (e.g., SRM 610). The external error in $^{206}Pb/^{238}U$ additionally incorporates the standard deviation of the mean of the discrimination-corrected $^{206}Pb^+/^{238}U[O_x]^+$ for a natural zircon standard. The analysis of $^{206}Pb^+/^{270}[UO_2]^+$ offers an improvement over

* Corresponding author. Fax: +1-613-995-7291.

E-mail address: rstern@nrcan.gc.ca (R.A. Stern).

measuring $^{206}Pb^+/^{238}U^+$ because variable discrimination is reduced or eliminated with respect to $^{254}[UO]^+/^{238}U^+$ and counting statistics are superior.

1. Introduction

Over the last two decades, the determination of $^{206}Pb–^{238}U$ ages in zircon ($ZrSiO_4$) using high mass resolution secondary ion mass spectrometry (HR-SIMS) has evolved to the point that it is now considered a routine procedure within several laboratories worldwide. Since the first high precision zircon dating study (Compston et al., 1984) there have been improvements to instrumentation, but only marginal reduction in analytical uncertainties in the $^{206}Pb/^{238}U$ ratios of unknowns. The typical analytical errors of individual ion probe spots of $\pm 1.0–3.0\%$ (1σ) reported in the literature are an order of magnitude larger than achievable by isotope dilution thermal ionization mass spectrometry (TIMS) of much larger (single or multigrain) samples. In conducting zircon geochronological studies using HR-SIMS, the benefit of microanalytical dating must be weighed against the comparatively poor $^{206}Pb–^{238}U$ age resolution.

The determination of a spot $^{206}Pb/^{238}U$ age with HR-SIMS is conceptually very simple: measure $^{206}Pb^+/^{238}U^+$, $^{206}Pb^+/^{254}[UO]^+$, or $^{206}Pb^+/^{270}[UO_2]^+$ (i.e., $^{206}Pb^+/^{238}U[^{16}O_x]^+$, where $x = 0$, 1, or 2), then correct the ratio for inherent discrimination of the Pb^+ and $^{238}U[^{16}O_x]^+$ ions in order to yield the true $^{206}Pb/^{238}U$. Consequently, in determining the analytical errors in spot $^{206}Pb/^{238}U$ ages, there are two main sources: the error in determining $^{206}Pb^+/^{238}U[^{16}O_x]^+$, and the error in making the discrimination correction. The methods of assessing the errors in $^{206}Pb^+/^{238}U[O_x]^+$ measurements differ in detail between laboratories, but all incorporate counting statistics and tend to yield similar results, typically $0.1–1.0\%$ (1σ), although surprisingly few critical assessments of their adequacy have been made. Estimates of the error related to discrimination correction are similar or higher, and may appear to differ between laboratories. For example, whereas the standard deviation of the

mean of $^{206}Pb^+/^{238}U[O_x]^+$ values about the reference curve has been used to estimate the uncertainty in the isotopic discrimination correction (Claoué-Long et al., 1995; Williams, 1998), in other cases the standard deviation has been utilized (Stern, 2000).

Regardless of how the spot $^{206}Pb/^{238}U$ errors in zircon analysis are derived, there is a critical reliance, both in their calculation and validation, upon homogeneous reference materials. From Kane (2001), we can calculate that for a claimed uncertainty of 1% in the $^{206}Pb/^{238}U$ value of an unknown, the uncertainty of this ratio in the reference material used for the calibration should be better than 0.3%. This is quite a stringent requirement for a U–Pb standard, particularly at the sampling scale of an ion microprobe, and in fact there is no reference material that has yet been proven homogeneous at the ion microprobe scale using an independent analytical technique. State-of-the-art U–Pb TIMS analyses of microgram quantities of reference materials still provide the most precise, accurate, and independent evidence of age homogeneity.

Stern (2001) reported U–Pb TIMS data for a natural zircon that appeared homogeneous to better than the required level for relatively large fragments. The results spurred additional analyses of much smaller fragments that are reported here, and which collectively indicate outstanding homogeneity within the sampling scale achievable with TIMS. In addition, U–Pb TIMS data were determined upon fragments of a well-known synthetic glass standard, the type of material that is equally, if not more, likely to be homogeneous at the ion microprobe scale. Using these reference materials, a critical analysis is presented on whether the errors used in this laboratory in determining spot $^{206}Pb^+/^{238}U[O_x]^+$ values and those associated with the discrimination correction are adequate. In addition, an improved procedure is presented for evaluating discrimination of U and Pb isotopes in zircon.

2. Discrimination of Pb^+ and U^+

The reason why discrimination occurs in the measurement of $^{206}Pb^+/^{238}U[O_x]^+$ in zircon is a fundamental question that relates mainly to the sputtering process, and only secondarily to the transmission of ions through the mass spectrometer. Simply stated, the issue is that $^{206}Pb^+/^{238}U^+$ values in zircon sputtered using a negative oxygen primary beam are typically $2-4\times$ greater than the values within the crystalline target. Countless mass spectrometric measurements of zircon show that the Pb^+ ions (both Pb and U ions are dominantly monovalent) occur almost entirely in the atomic state, whereas $^{254}[UO]^+$ and $^{270}[UO_2]^+$ ions are dominant over the atomic ion species ($^{254}[UO]^+>$ $^{270}[UO_2]^+>^{238}U^+$). The predominance of UO_x^+ ions compared with U^+ in zircon is consistent with sputtering data for metals showing that the MO^+/M^+ values correlate positively with the M^+-O bond dissociation energy (Wittmaack, 1979). The U^+-O bond dissociation energy is about $4\times$ that of Pb^+-O. It appears that the energy state of the sputtered region (considered to be just above the sample surface) is high enough to de-stabilize lead oxides, but not so energetic as to cause total dissociation of UO_x^+ ions. Although the secondary ion yields for $^{206}Pb^+$ are enhanced over $^{238}U^+$, the ratio of the total number of $^{206}Pb^+$ ions to the total number of $^{238}U^+$ ions occurring within atomic *plus* oxide species [i.e., $^{206}Pb^+/(^{238}U^+ + ^{254}[UO]^+ + ^{270}[UO_2]^+)$] is estimated to be about one-third of that existing within the zircon, i.e., *less* than the target ratio. In other words, uranium secondary species in total are ionized more readily than Pb in the presence of a negative oxygen beam.

A major complication in estimating the extent of discrimination between $^{206}Pb^+$ and $^{238}U[O_x]^+$ for a particular spot analysis is that, for poorly understood reasons, the discrimination usually varies between analytical spots on zircons. In many cases it is clear that time-dependent instrumental 'drift' is not a factor, and that, all other things being equal, the variations are more likely to relate to inhomogeneities in the surface electrostatic properties of the mount, differences in mineral composition, or differences in the way that secondary ions are collected and transmitted. The precise determination of the U–Pb discrimination that existed for a given spot has resisted theoretical treatment, but can be accomplished if the pattern of absolute and relative variation in the discrimination is determined empirically.

There are differences in the procedures, parameters, and assumptions used by different laboratories to accomplish the task of deducing the pattern of relative and absolute U–Pb discrimination. The common approach is to establish or at least refine, through concurrent analysis of a homogeneous reference material, the best-fit functional relationship between the desired $^{206}Pb^+/^{238}U[O_x]^+$ ratio and an isotopic ratio involving uranium species. Traditionally used are $^{206}Pb^+/^{238}U^+$ and $^{254}[UO]^+/^{238}U^+$ (e.g., Compston et al., 1984; Hinthorne et al., 1979; Ludwig, 2001a), and less commonly $^{206}Pb^+/^{254}[UO]^+$ (Compston, 2000) and $^{270}[UO_2]^+/^{238}U^+$ (Whitehouse et al., 1997). In cases where $^{206}Pb^+/^{238}U[O_x]^+$ is considered dependent upon another isotopic ratio such as $^{254}[UO]^+/^{238}U^+$, there is almost always an assumption made about the form of the functional relationship, i.e., whether linear, quadratic, power, etc. For example, in the 'SQUID' data processing approach (Ludwig, 2001a), a power curve form ($^{206}Pb^+/^{238}U^+ = A \cdot {}^{254}[UO]^+/^{238}U^{+E}$) and fixed exponent value (E, normally 2.0) are assumed, and repeat analyses of the reference material are used to determine the value of A. The ratio of this value of A for the standard with the analagous value calculated from an individual analysis of an unknown supplies the discrimination-corrected proportionality of their $^{206}Pb/^{238}U$ values.

Despite widespread use, the typical correlations observed between $^{254}[UO]^+/^{238}U^+$ and $^{206}Pb^+/^{238}U[O_x]^+$ in zircon are not well understood, and in some cases misinterpreted. Causes of coupled variations in $^{254}[UO]^+/^{238}U^+$ and $^{206}Pb^+/^{238}U^+$, for example, have included changes in spot temperature and electron density (Hinthorne et al., 1979) and variations in oxygen fugacity (Whitehouse et al., 1997), both potentially affecting the relative extent of uranium speciation with oxygen. Changes in ion energy due to sample charging is another explanation for the correlated behaviour of these isotope ratios (e.g., Holliger, 1992; Whitehouse et al., 1997).

An extensive examination of instrumental factors that might explain the relative dependence of $^{206}Pb^+/^{238}U[O_x]^+$ species on $^{254}[UO]^+/^{238}U^+$ was carried out as background to this study. The results indicate that the precise relationship between $^{254}[UO]^+/^{238}U^+$ and $^{206}Pb^+/^{238}U[O_x]^+$ is governed largely by sample char-

ging effects and the width of the energy window, coupled with the particular way that secondary ions are transmitted to the collector. No two instruments or analytical conditions will necessarily display exactly the same relationships between $^{254}[UO]^+/^{238}U^+$ and $^{206}Pb^+/^{238}U[O_x]^+$, but consistently it is found that the dependence on $[UO]^+/^{238}U^+$ decreases in the order $^{206}Pb^+/^{238}U^+ > ^{206}Pb^+/^{254}[UO]^+ > ^{206}Pb^+/^{270}[UO_2]^+$. Below it will be shown that $^{206}Pb^+/^{270}[UO_2]^+$ exhibits no functional relationship with $[UO]^+/^{238}U^+$, and thus apparently no quantifiable variation in discrimination. In all cases, however, the assumption made about the nature of the functional relationship, or the absence of one, is deduced from more exhaustive data sets, and only validated by the smaller data sets collected during routine work. In no case should it be assumed a priori that the functional relationships assumed for one lab will necessarily and exactly apply to another.

Table 1
ID-TIMS U–Pb analytical data for z6266 zircon

Fraction identification	Weight (mg)	U (ppm)	Th (ppm)	Pb (ppm)	Th/U[a] (wt.)	Common Pb[b] (pg)	$^{207}Pb/^{204}Pb$	Radiogenic ratios[c] $\pm 2\sigma$(absolute)[d]		
								$^{207}Pb/^{235}U$	$\pm^{207}Pb/^{235}U$	$^{206}Pb/^{238}U$
GSC-M	0.0010					6.7	72	0.7327	0.0033	0.09050
GSC-Q	0.0010					8.0	56	0.7371	0.0044	0.09063
GSC-K	0.0012					29.0	30	0.7385	0.0156	0.09056
GSC-L	0.0015					10.0	70	0.7371	0.0046	0.09062
GSC-O	0.0015					11.1	59	0.7344	0.0042	0.09046
ROM-ZIR16 (up20–133)	0.0040					1.7	969	0.7362	0.0022	0.09066
ROM-ZIR15 (up20–131)	0.0050					2.0	766	0.7374	0.0020	0.09085
ROM-ZIR17 (up20–135)	0.0050					2.0	1032	0.7370	0.0022	0.09080
ROM-ZIR14 (up20–129)	0.0070					1.3	1974	0.7347	0.0021	0.09053
ROM-ZIR13 (up20–127)	0.0070					1.4	1671	0.7364	0.0020	0.09070
ROM-ZIR10 (mean of two solution aliquots)	0.0100						8330	0.7363	0.0013	0.09062
ROM-ZIR11 (mean of five solution aliquots)	0.0103					0.1	5056	0.7347	0.0009	0.09048
ROM-ZIR12 (mean of three solution aliquots)	0.0103						2758	0.7360	0.0012	0.09061
GSC-U	0.0234	942	209	82.7	0.2223	4.1	1779	0.7340	0.0018	0.09047
GSC-G	0.0417	895	199	78.5	0.2220	4.5	2796	0.7345	0.0014	0.09049
GSC-D	0.0525	889	197	78.2	0.2211	2.4	6579	0.7361	0.0014	0.09070
GSC-F	0.0612	896	196	78.6	0.2188	4.4	4154	0.7351	0.0014	0.09056
GSC-C	0.0618	871	191	76.5	0.2188	2.5	7181	0.7357	0.0015	0.09065
GSC-A	0.0786	920	204	80.8	0.2217	1.6	15274	0.7348	0.0014	0.09054
GSC-E	0.0901	910	200	80.0	0.2193	2.8	9676	0.7359	0.0014	0.09065
GSC-B	0.1198	958	212	84.2	0.2215	3.5	10920	0.7352	0.0015	0.09059
GSC-H	0.1390	933	207	82.0	0.2220	6.4	6732	0.7347	0.0015	0.09053

[a] Th/U calculated from radiogenic $^{208}Pb/^{206}Pb$ and $^{207}Pb/^{206}Pb$; Th abundance calculated from Th/U and U.

[b] Common Pb (pg) refers to the total amount of common Pb (pg) measured in the analysis.

[c] Atomic ratios corrected for Pb and U blank, fractionation, and initial common Pb (Stacey and Kramers, 1975).

[d] Uncertainties are calculated by numerical propagation of all known sources of error.

[e] Percent discordance along a line to zero age.

3. Experimental

3.1. Reference materials

The zircon standard used in this study was sample z6266 (formerly 'BR266') comprising clear, colour-less, glassy fragments obtained from a single Sri Lankan megacryst (Stern, 2001). Powder X-ray diffraction lattice parameters are consistent with a small amount of accumulated radiation damage. Major and trace element analysis of randomly selected fragments of z6266 using various microprobe methods (SHRIMP, electron microprobe, laser ablation ICP-MS, TIMS) indicate remarkable chemical homogeneity (Stern, 2001). The standard deviation of abundance measurements for most elements, including U and Th, at all scales is $\pm 2-5\%$. TIMS isotope dilution data (Table 1) for nine large fragments (>23 μg), for which

$\pm^{206}Pb/$ ^{238}U	Correlation coefficient	$^{207}Pb/$ ^{206}Pb	$\pm^{207}Pb/$ ^{206}Pb	$^{208}Pb/$ ^{206}Pb	Apparent Ages (Ma) $\pm 2\sigma$						$\%D^{e}$
					$^{207}Pb/$ ^{235}U	$\pm^{207}Pb/$ ^{235}U	$^{206}Pb/$ ^{238}U	$\pm^{206}Pb/$ ^{238}U	$^{207}Pb/$ ^{206}Pb	$\pm^{207}Pb/$ ^{206}Pb	
0.00024	0.645	0.058722	0.000206		558.1	2.0	558.5	1.4	556.8	7.6	− 0.30
0.00031	0.541	0.058983	0.000300		560.7	2.6	559.3	1.8	566.4	11.0	1.30
0.00042	0.590	0.059146	0.001107		561.5	9.1	558.8	2.5	572.5	40.2	2.50
0.00040	0.565	0.058994	0.000310		560.7	2.7	559.2	2.4	566.9	11.4	1.40
0.00031	0.633	0.058877	0.000260		559.1	2.5	558.3	1.8	562.5	9.6	0.80
0.00025	0.891	0.058896	0.000080		560.2	1.3	559.4	1.5	563.3	3.0	0.70
0.00022	0.857	0.058866	0.000084		560.9	1.2	560.6	1.3	562.2	3.1	0.30
0.00026	0.879	0.058867	0.000086		560.6	1.3	560.2	1.5	562.2	3.2	0.40
0.00023	0.938	0.058860	0.000058		559.3	1.2	558.7	1.4	561.9	2.1	0.60
0.00023	0.915	0.058883	0.000066		560.3	1.2	559.7	1.3	562.8	2.4	0.60
0.00015	0.958	0.058932	0.000030		560.2	0.8	559.2	0.9	564.6	1.1	0.95
0.00010	0.935	0.058889	0.000026		559.3	0.5	558.4	0.6	563.0	1.0	0.82
0.00015	0.577	0.058909	0.000089		560.1	0.7	559.1	0.9	563.7	3.3	0.82
0.00019	0.901	0.058840	0.000062		558.9	1.1	558.3	1.1	561.2	2.3	0.50
0.00016	0.953	0.058870	0.000036	0.069222	559.2	0.8	558.4	0.9	562.3	1.4	0.69
0.00016	0.962	0.058858	0.000048	0.068946	560.1	0.8	559.7	0.9	561.9	1.8	0.39
0.00016	0.951	0.058876	0.000037	0.069199	559.6	0.8	558.8	0.9	562.5	1.4	0.66
0.00016	0.952	0.058866	0.000036	0.068227	559.9	0.9	559.4	0.9	562.2	1.4	0.50
0.00015	0.964	0.058864	0.000032	0.069110	559.4	0.8	558.7	0.9	562.1	1.2	0.60
0.00016	0.964	0.058879	0.000032	0.068373	560.0	0.8	559.4	0.9	562.6	1.2	0.58
0.00016	0.966	0.058863	0.000033	0.069064	559.6	0.9	559.0	1.0	562.0	1.2	0.54
0.00017	0.967	0.058865	0.000032	0.069223	559.3	0.9	558.7	1.0	562.1	1.2	0.62

weighing errors are negligible, yield a mean U concentration of 903 ± 23 ppm (1 standard deviation, S), total Pb = 79 ± 2 ppm, and model Th = 199 ± 6 ppm. The well-developed crystallinity and chemical homogeneity minimize potential effects due to matrix variations. The U–Pb TIMS isotopic data are reported and discussed below.

Also utilized in this study was the Si–Na–Ca–Al–O reference glass of the National Institute of Standards and Technology (NIST), standard reference material (SRM) 610 (Reed, 1992). The certified (TIMS) abundances are 461.5 ppm U, 457.2 ppm Th, and 426 ppm Pb (Reed, 1992), although recent compilations suggest values that deviate slightly from these certified values (Pearce et al., 1997; Rocholl et al., 1997, 2000). The isotopic composition of the common Pb in the glass has been determined very precisely by TIMS using a double spike technique (Woodhead and Hergt, 2001). Using the data of Rocholl et al. (2000) and Woodhead and Hergt (2001), the $^{206}Pb/^{238}U$ value for SRM 610 can be calculated as 0.2569.

The homogeneity of Pb, U, and Th abundances in SRM 610 was established on a bulk scale as part of the original certification procedure (Reed, 1992). Utilizing a Cameca IMS-4f ion microprobe, Hinton et al. (1995) demonstrated that there was no detectable heterogeneity in the abundances of refractory lithophile elements, including U, Th, and Pb, at all sampling scales. For that study, the standard deviations of U, Th, and Pb were 1.2%, 1.8%, and 7.6%, respectively, similar to or less than expected from counting statistics. Additional ion probe data (Rocholl et al., 2000) confirm homogeneity in Th and other elements. Although these previous studies did not pay special attention to the homogeneity in U, Th, and Pb in SRM 610, in all cases, micro-scale trace element heterogeneity within a chip was undetectable. The differences in the abundances of many trace elements in a single chip are unlikely to exceed 1% (Hinton et al., 1995), and the variations in the ratios of these elements (e.g., Pb/U, Th/U) are likely to be much smaller. The homogeneity in Pb/U and Th/U in SRM 610 used in this study was confirmed through TIMS analyses (see below).

3.2. Mounts

The HR-SIMS experiments were carried out using two separate grain mounts. One (#IP222) comprised

61 fragments, 60–100 μm in dimension, of z6266 zircon spaced more or less evenly within the mount 'bullseye' (Fig. 2). The bullseye occupies the inner 1.5 cm diameter of the grain mount, where edge effects from the steel holder are minimized (see further discussion below). The fragments are believed to be oriented randomly with respect to the zircon structural axes. Two to four separate spot analyses were acquired from each fragment during one analytical session lasting 25 h, yielding a total of 162 analyses (experiment IP222.1). Following a 2-month hiatus, the mount was lightly polished to eliminate these pits and a further 63 analyses acquired in a second analytical session lasting 12 h (experiment IP222.2). In the latter, only a subset of the grains was re-analyzed from the inner 1 cm diameter of the bullseye.

A second mount (IP109) included a single, 1.5×2.5 mm fragment of SRM 610 glass located within the bullseye, from which 143 separate spot analyses were acquired in a systematic grid pattern, spaced ∼ 100 μm apart.

4. Analytical techniques

4.1. Error analysis and terminology

Concordia diagrams, weighted means, mean square of weighed deviates (MSWD), probability of fit (P), and excess scatter values were calculated using ISO-PLOT-Ex (Ludwig, 2001b). The standard deviation of a set of data (i.e., dispersion) is termed S, whereas the standard deviation of the mean (= standard error = $S/\sqrt{n}$) is termed 'SE'. The 68% and 95% confidence intervals are termed σ and 2σ. The mean square of weighted deviates (MSWD)=$\{\Sigma_i^n \ ((A_i - A)/\sigma_i)^2)\}/(N-1)$, where A_i, A, σ_i, and N are the individual datum value, mean or predicted value, datum error, and number of data, respectively.

Three levels of error estimates can be defined for individual spot HR-SIMS analyses as illustrated in Fig. 1. The most basic error estimate is termed here the *within-spot* ratio error. It is simply the uncertainty in a ratio at a particular spot, such as $^{206}Pb^+/^{238}U^+$ or $^{254}[UO]^+/^{238}U^+$, that may be used in subsequent age calculations. Variations in the intensity of individual isotopes will normally occur during an analysis, due
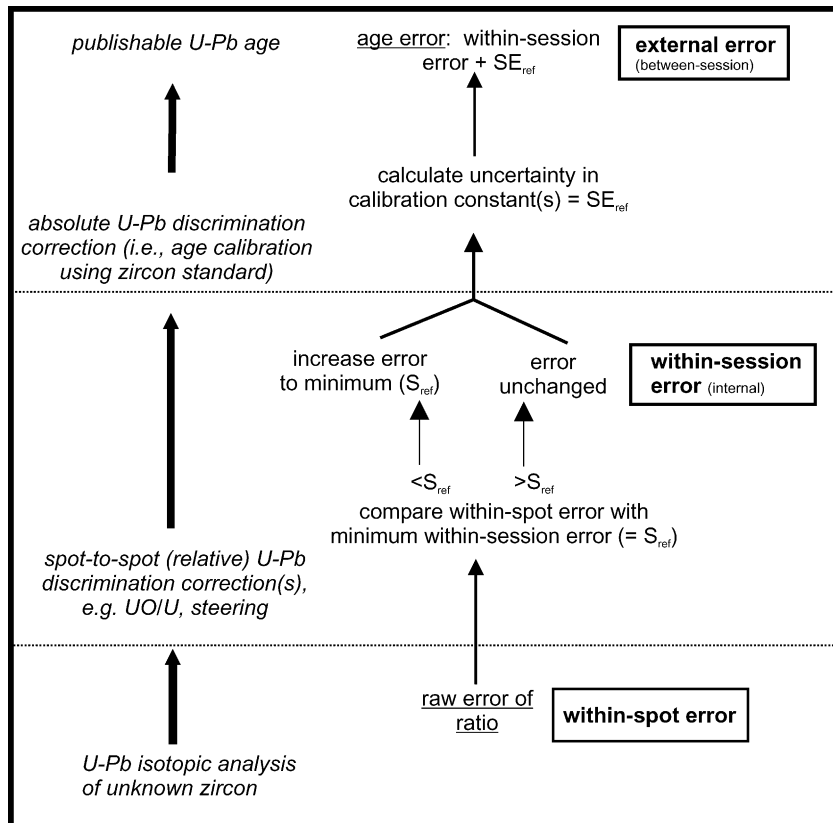
Fig. 1. Flow chart illustrating the transformation of raw isotopic ratios to ^{206}Pb/^{238}U ages. On the left, the sequence includes collection of raw isotopic ratios, correction for any relative differences in discrimination, and then finally correction for absolute discrimination by comparison with a standard. On the right, there are parallel uncertainties in the ratios that increase through the sequence. The least uncertainty is the *within-spot* error associated with the raw ratio. If spots are to be compared, however, we speak of *within-session* errors that have a minimum value defined by the reproducibility of a standard (S_{ref}). Conversion to absolute ages also introduces an additional error associated with the uncertainty in the calibration constants for the standard (SE_{ref}). The cumulative error is termed the *external error*, which is the one usually quoted for publication. See text for details.

mainly to uncontrollable primary beam instability and systematic, time-dependent variations in ion yields. Some of these effects can be reduced by simultaneous monitoring and normalization to the total secondary ion current measured prior to the object slit ('secondary beam monitor'). Normally, the secondary-beam-normalized counts vs. time trend for an isotope is either unchanging or approximates a slight linear increase or decrease. Least-squares regression of the time series provides the basis for calculating the isotope count rate at a given time in the analysis, referred to as the 'snapshot' method (Williams, 1998). Here, the isotope count rates were determined at the half-way point of the analysis, equivalent to the

vertical center of the pit. Isotope ratios are calculated from pairs of isotope count rates.

The minimum within-spot error is limited by ion counting statistics, but other sources of within-analysis variability (see below) typically augment the counting error estimate. The larger of the following two error calculations defines the within-spot error for the midpoint count rate of individual isotopes. The first is a determination of the counting statistical error, i.e.,

$$\pm \sigma = cps_{mid} / \sqrt{n_{tot}}$$

where cps_{mid} refers to the count rate at the midpoint and n_{tot} is the total number of counts collected.

The second count rate error estimate is derived from the linear regression of the time series as follows (after Mendenhall and Sincich, 1995; York, 1969):

$$\pm\sigma = S * t_{0.16} * \sqrt{[1/N]} * \sqrt{MSWD}$$

where S is the standard deviation (in cps) about the regression curve, $t_{0.16}$ is the one-tailed Student's t value for $N-2$ degrees of freedom, N is the number of scans, and MSWD is ≥ 1. The errors of individual scans in the MSWD calculation are derived from simple counting statistics. Isotope count rate errors are summed quadratically to yield the within-spot ratio errors.

The second level of uncertainty for an analysis may be termed the *within-session* ('internal') error (Fig. 1). This error refers to the uncertainty of a single spot isotope ratio determination made during an individual analytical session. The within-session error allows isotopic ratios or ages of spots collected during the session to be compared, and incorporates the within-spot errors and any errors related to corrections for variable discrimination. The error in making the absolute discrimination correction, required to calculate accurate $^{206}Pb/^{238}U$ ages, is not incorporated in the within-session age errors.

The third and highest level of uncertainty for an analysis may be termed the *external* (or between-session) error (Fig. 1), in which the within-session age error is further augmented by uncertainty in the absolute U–Pb discrimination correction made in the age calculation. The latter reflects the uncertainties in the true age assumed for the standard actually utilized during the session, which in turn is related to the homogeneity of the standard and the number of analyses collected during the session. The external error allows ages between analytical sessions to be compared, and is the uncertainty that should normally be used in the publication of results, although within-session age errors may be justified in cases where the relative age distinctions within a particular session are considered paramount. The methods of determining the within-session and external errors form much of the focus of this paper, and are summarized in Section 6.

A factor termed 'excess scatter' is used here to quantify the extent of data dispersion beyond assigned errors, and is provided by ISOPLOT as the 'constant external error' value in the weighted mean algorithm.

The assumption is that a perfect data set will have an MSWD of unity, and higher values indicate that some unaccounted variability exists. For simplicity it is assumed that all errors, rather than a particular subset of errors, for such data are too low. A small error is incrementally added (quadratically) to all of the assigned individual errors and the weighted mean and MSWD recalculated. The process is repeated until the MSWD is reduced to exactly 1.0. The excess scatter is the cumulative error added to each datum, and is expressed as a percentage of the mean.

4.2. HR-SIMS

4.2.1. Instrumentation

A SHRIMP II ion microprobe housed at the Geological Survey of Canada, Ottawa was used in this study (Stern, 1997). Mass-resolved O^- primary ions were generated in a hollow Ni cathode and projected at 10 keV onto the target at a 45° incidence angle. The experiments employed 20 μm diameter spots of uniform beam density ($\sim$ 10 nA), giving a sputtering rate of about 5 μm/h. Positive secondary ions were extracted at 10 kV total potential, with the first extraction electrode at 750 V, and subsequently focussed on the object slit (110 μm) using a quadrupole lens triplet. The 1272 mm radius electostatic analyzer (ESA) was held at 950 V. The energy window, located on the ESA focal plane, was set to a width of 2.5 mm, allowing an energy bandpass of 20 eV. Mass dispersion and refocussing onto the image (collector) slit of 100 μm width was performed using a laminated electromagnet of 1 m radius. Secondary ion arrival rates were measured using a single electron multiplier coupled to an ion counting system with a deadtime of 25 ns. Under these operating conditions, the 1% mass resolution was 5500 and ^{206}Pb sensitivity for zircon about 9 cps/ppm/nA O^-. Approximately 0.3% of all Pb atoms sputtered arrive at the detector (Stern, 1997).

Diamond-polished sections of the mineral specimens were exposed on standard 2.5 cm diameter epoxy grain mounts. The mount surfaces were cleaned, evaporatively coated with 10 nm of high-purity Au, and a conducting steel ring was clamped to the outer edges of the epoxy disk (Fig. 2). The mounts were held at high vacuum for several hours prior to analysis.
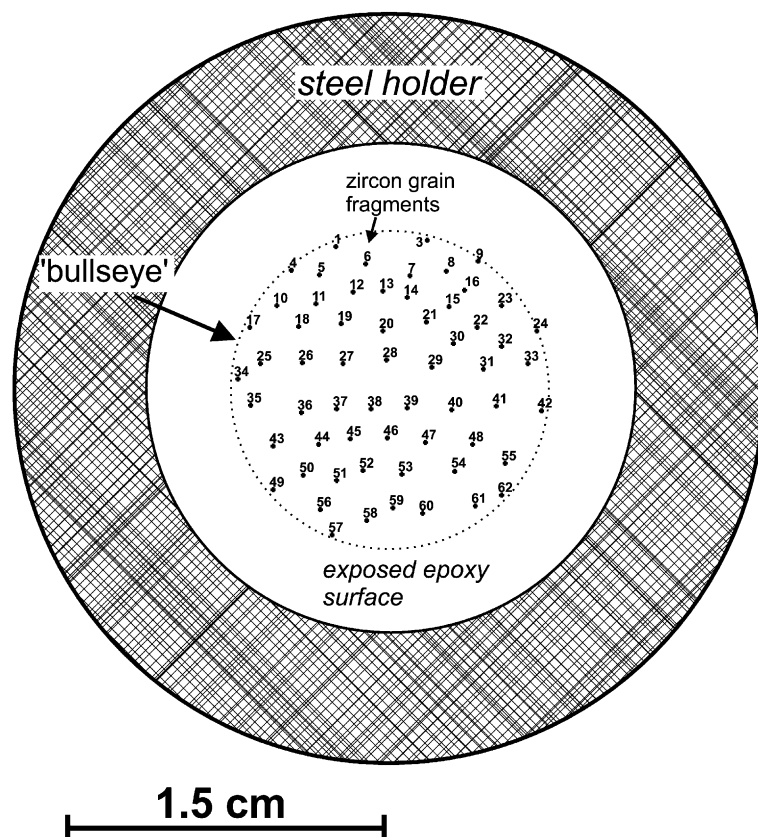
Fig. 2. Sketch of grain mount IP222 exposing fragments (numbered) of z6266 zircon within the 1.5-cm diameter 'bullseye' (dashed circle). Within this region the secondary ion steering effects are minimized, but they are not zero (see Fig. 7). The diameter of the entire exposed mount surface is 2.2 cm.

4.2.2. Data collection

Individual zircon U–Pb measurements consisted of sequential monitoring (six scans) of the count rates of the following isotopes: $^{196}[Zr_2O]^+$, $^{204}Pb^+$, background, $^{206}Pb^+$ [$^{207}Pb^+$ and $^{208}Pb^+$ omitted in some experiments], $^{238}U^+$, $^{248}[ThO]^+$, $^{254}[UO]^+$, $^{270}[UO_2]^+$. An 'analytical session' is defined here as a period of time in which all analyses were carried out from a single sample mount under stable analytical conditions, i.e., primary beam intensity and imaging, secondary extraction voltage, energy bandpass, electron multiplier voltage, etc., are constant. Only minor changes to the path of the secondary ion beam (termed deflections or steering) occurred between spot positions in order to maximize secondary ion count rates, in particular the use of $^{270}[UO_2]^+$ in this study. These adjustments involved deflections of the secondary ion beam in the horizontal and vertical coordinates (y- and z-axes, respectively) within the source chamber, prior to the ESA.

The y-axis deflections comprise two separate actions by the analyst. The first action places a bias voltage on one of three quadrupole lenses, and is termed 'quadrupole y-steering', which deflects the secondary ions horizontally prior to the object slit. The second adjustment, termed 'pre-alpha (slit) y-steering', places a bias voltage on vertically oriented plates that deflect the ion image of the object slit prior to entry into the ESA, whose acceptance is limited by entry ('alpha') slits. The alpha slits are normally open as far as possible in the y-direction, but a certain extent of beam truncation is required to maintain adequate ESA

performance and mass resolution. In this paper, the sum of the optimized quadrupole lens and deflection voltages for the y-axis components is termed 'net y-steering'. Analogous deflections exist for the z-direction (vertical), but in this study only the 'pre-alpha (slit) z-steering' component was adjusted.

One might ask why it is necessary to alter the secondary ion steering parameters at all, given the fact that the target is always at the same location relative to the first extraction electrode (i.e., coaxial with the secondary column). The explanation is that the trajectory of secondary ions from the surface of the mount into the secondary column is affected by nearby surface features. Any significant surface relief, such as from deep craters or channels, or previously analyzed spots, may perturb the secondary ion pathway, presumably by disruption of the electrostatic surface potentials. The circular steel mount holder whose edge is located 1.1 cm from the center of the mount exerts a particularly important effect, as will be discussed below.

4.3. TIMS

Fragments of z6266 zircon were analyzed at the Geological Survey of Canada (GSC), Ottawa laboratories and at the Royal Ontario Museum (ROM), Toronto. The analytical procedures are based on the technique of Krogh (1973), with various modifications, including the use of mixed $^{205}Pb-^{235}U$ (ROM) and $^{205}Pb-^{233}U-^{235}U$ (GSC) spikes and small anion exchange columns (see Amelin, 1998; Amelin et al., 1994; Parrish et al., 1987). The U–Pb isotopic composition of these spikes was calibrated independently within each laboratory. The Pb isotopic ratios were corrected for fractionation of 0.09 (± 0.054) %/amu (2σ, GSC) and 0.100 (± 0.076) %/amu (ROM) based upon periodic analyses of NIST SRM 981 (natural Pb metal). The U-isotopic ratios were corrected for fractionation using $^{233}U/^{235}U$ (GSC) and 0.100 (± 0.052) %/amu (ROM) based upon analyses of the New Brunswick Laboratory U500 Certified Reference Material. Procedural blanks for U were < 0.2 pg and for Pb were within 2–6 pg (GSC) and 0.2–1.0 pg (ROM). Residual common Pb was subtracted using terrestrial compositions (Stacey and Kramers, 1975). Decay constants were 1.55125×10^{-10} (^{238}U) and 9.8485×10^{-10} (^{235}U) (Steiger and Jäger, 1977).

5. Results

5.1. TIMS results

The TIMS U–Pb data for z6266 zircon are presented in Table 1. The weighted mean of 22 TIMS $^{206}Pb*/^{238}U$ measurements of randomly selected fragments of z6266 zircon ranging in mass from 1 to 139 µg are indistinguishable within analytical error, at 0.090583 ± 0.000038 (2σ; MSWD = 1.1, probability of fit, $P = 0.31$), equivalent to an age of 559.0 ± 0.2 Ma (2σ; Fig. 3a,b). The weighted mean of 22 $^{207}Pb*/^{206}Pb*$ measurements is 0.058878 ± 0.000011 (2σ; MSWD = 1.2, $P = 0.27$), equivalent to an age of 562.6 ± 0.4 Ma (2σ). The weighted average of the analyses is shown as the small shaded ellipse in Fig. 3(a) and is 0.67% discordant relative to the origin. Nevertheless, the probability that the data are concordant is 0.15 (MSWD = 2.1) when the decay constant errors are included (Ludwig, 2001b).

Fig. 3(c) shows a probability density plot (after Silverman, 1986) of the TIMS $^{206}Pb/^{238}U$ ratios, illustrating a unimodal, Gaussian distribution with a slight positive skew. The range of $^{206}Pb/^{238}U$ ratios is $\pm 0.4\%$ about the mean, the standard deviation is $\pm 0.092\%$, and the mean individual error is $\pm 0.08\%$. It is important to note that there is no correlation between the mass of the fragments and the measured $^{206}Pb/^{238}U$ ratios (Fig. 3b). The mean Th/U is 0.221 ± 0.001 (1S).

The simplest interpretation of the TIMS data is that zircon z6266 is isotopically homogeneous at volumes of 2×10^5 µm³ or greater, the approximate volume of the smallest fragment analyzed. Isotopic heterogeneities, if they exist, are either absent or occur at significantly finer scale than is possible to examine with the TIMS method. The absence of correlation between age and size argues, however, against the existence of size-related isotopic heterogeneities. Variations in the $^{206}Pb/^{238}U$ ages outside of error would be anticipated if the zircon had suffered Pb-loss, but whether or not the zircon is discordant is equivocal. A similar pattern of apparent slight discordance was found for another ion probe standard, SL13, also a Sri Lankan zircon (Roddick and van Breemen, 1994; Claoué-Long et al., 1995). Roddick and van Breemen (1994) suggested that the slight discordance was not a result of Pb-loss but possibly the incorporation of an excess of ^{231}Pa, an intermediate daughter in the ^{235}U
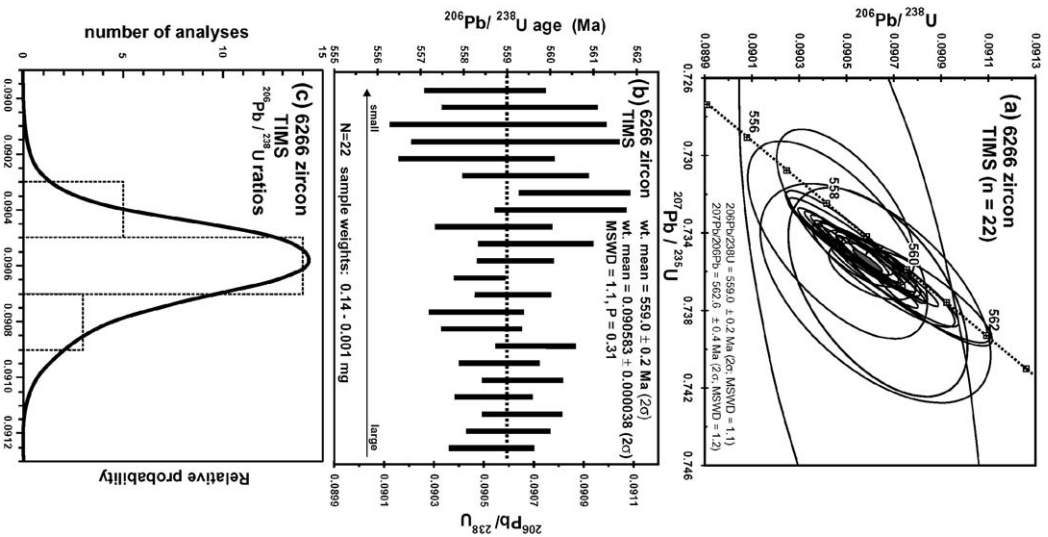
Fig. 3. TIMS U–Pb isotopic results for variably sized fragments of z6266 zircon obtained from two independent laboratories (see Table 1 for data). (a) U–Pb concordia diagram showing slight apparent discordance; error ellipses are at 95% confidence level; shaded ellipse is weighted average of all data. (b) Bar graph of ^{206}Pb/^{238}U ratios (95% confidence level), and equivalent ages, relative to the weighted mean. (c) Probability distribution and histogram of ^{206}Pb/^{238}U ratios. Note the Gaussian form of the curve, which is considered to be the limiting distribution of ^{206}Pb/^{238}U for this zircon.

decay chain, during crystallization, resulting in unsupported radiogenic ^{207}Pb.

Even if one accepts that heterogeneities in ^{206}Pb/^{238}U might exist at the 10^2 μm^3 volumes of a typical ion probe analysis, the fact that the TIMS ^{206}Pb/^{238}U

Table 2
ID-TIMS U–Pb analytical data for NIST 610 glass

Fraction	Weight (μg)	Pb/U[a] (wt.)	Th/U[a] (wt.)	±2σ (%)	Th/Pb[a] (wt.)	±2σ (%)	^{206}Pb/^{204}Pb[b]	±2σ (%)	^{207}Pb/^{204}Pb[b]	±2σ (%)	^{208}Pb/^{204}Pb[b]	±2σ (%)	^{238}U/^{204}Pb[c]	±2σ (%)	^{206}Pb/^{238}U[c]	±2σ (%)	^{207}Pb/^{235}U[c]	±2σ (%)	Error correlation coefficients		
																			Pb 6/4–7/4	Pb 6/4–8/4	Pb/U 6/38–7/35
UP24-020	3	0.9214	0.9958	5.33	1.0808	5.32	17.035	0.10	15.489	0.14	36.929	0.19	66.405	0.28	0.2565	0.26	97.451	0.27	0.972	0.953	0.981
UP24-021	4	0.9207	0.9853	0.53	1.0702	0.45	17.043	0.10	15.500	0.14	36.951	0.18	66.494	0.32	0.2563	0.31	97.388	0.31	0.970	0.969	0.985
UP24-023	8	0.9202	0.9876	0.52	1.0731	0.41	17.051	0.10	15.506	0.14	36.981	0.19	66.566	0.35	0.2561	0.34	97.323	0.34	0.988	0.946	0.991
UP24-025	5	0.9227	0.9894	0.44	1.0723	0.41	17.039	0.09	15.495	0.14	36.951	0.19	66.342	0.21	0.2568	0.19	97.580	0.19	0.966	0.948	0.959
UP24-026	12	0.9223	0.9846	0.46	1.0676	0.43	17.027	0.11	15.491	0.16	36.960	0.21	66.359	0.29	0.2566	0.26	97.531	0.27	0.910	0.870	0.962
UP24-027	6	0.9221	0.9881	0.51	1.0717	0.42	17.042	0.10	15.496	0.14	36.951	0.18	66.389	0.32	0.2567	0.31	97.518	0.31	0.987	0.967	0.989
UP24-028	10	0.9207	0.9874	0.55	1.0725	0.42	17.051	0.10	15.503	0.14	36.953	0.18	66.507	0.38	0.2564	0.37	97.389	0.37	0.975	0.973	0.991
UP24-029	9	0.9228	0.9838	0.45	1.0662	0.42	17.057	0.10	15.515	0.14	36.993	0.18	66.408	0.20	0.2568	0.18	97.613	0.18	0.981	0.976	0.965

[a] Total elemental abundance ratios.

[b] Atomic ratios corrected for analytical blank and mass fractionation.

[c] Atomic ratios corrected for Pb and U blank, fractionation, and ^{238}U/^{235}U = 417.8 measured in this study.

Table 3
Raw SHRIMP isotopic data ($\pm 1\sigma$) for NIST SRM 610 glass, mount IP109

Analysis number	$^{208}Pb/^{206}Pb$	$\pm^{208}Pb/^{206}Pb$	$^{206}Pb/^{238}U$	$\pm^{206}Pb/^{238}U$	$^{254}U/^{238}U$	$\pm^{254}U/^{238}U$	$^{270}U/^{238}U$	$\pm^{270}U/^{238}U$	$^{208}Pb/^{248}Th$	$\pm^{208}Pb/^{248}Th$	$^{206}Pb/^{254}U$	$\pm^{206}Pb/^{254}U$	$^{248}Th/^{254}U$	$\pm^{248}Th/^{254}U$	$^{270}U/^{254}U$	$\pm^{270}U/^{254}U$	$^{206}Pb/^{270}U$	$\pm^{206}Pb/^{270}U$
1	2.186	0.015	0.2509	0.0012	2.628	0.013	0.6884	0.0030	0.2107	0.0014	0.09547	0.00055	0.9908	0.0053	0.2619	0.0014	0.3645	0.0019
2	2.179	0.013	0.2427	0.0017	2.678	0.026	0.6909	0.0040	0.2013	0.0010	0.09063	0.00091	0.9813	0.0092	0.2580	0.0024	0.3513	0.0022
3	2.163	0.011	0.2446	0.0016	2.655	0.018	0.6914	0.0043	0.2028	0.0011	0.09212	0.00048	0.9822	0.0054	0.2604	0.0013	0.3537	0.0016
4	2.139	0.010	0.2481	0.0013	2.671	0.015	0.6922	0.0036	0.2044	0.0015	0.09289	0.00042	0.9723	0.0072	0.2592	0.0011	0.3584	0.0015
5	2.161	0.010	0.2499	0.0012	2.661	0.014	0.6903	0.0027	0.2062	0.0011	0.09392	0.00056	0.9845	0.0063	0.2595	0.0014	0.3620	0.0017
6	2.183	0.010	0.2487	0.0011	2.649	0.011	0.6796	0.0030	0.2068	0.0013	0.09389	0.00044	0.9913	0.0065	0.2566	0.0012	0.3659	0.0018
7	2.158	0.014	0.2469	0.0014	2.622	0.011	0.6853	0.0034	0.2041	0.0010	0.09417	0.00057	0.9959	0.0044	0.2614	0.0014	0.3602	0.0024
8	2.146	0.009	0.2501	0.0011	2.653	0.013	0.6936	0.0031	0.2043	0.0008	0.09424	0.00047	0.9899	0.0049	0.2614	0.0013	0.3605	0.0016
9	2.179	0.010	0.2508	0.0017	2.671	0.021	0.7001	0.0050	0.2085	0.0010	0.09391	0.00055	0.9812	0.0057	0.2621	0.0016	0.3583	0.0018
10	2.157	0.015	0.2469	0.0011	2.692	0.012	0.7040	0.0040	0.2006	0.0015	0.09169	0.00039	0.9859	0.0049	0.2615	0.0014	0.3507	0.0019
11	2.167	0.010	0.2429	0.0010	2.679	0.011	0.6955	0.0027	0.2006	0.0009	0.09066	0.00041	0.9789	0.0041	0.2596	0.0011	0.3492	0.0015
12	2.173	0.010	0.2473	0.0010	2.654	0.020	0.6913	0.0028	0.2044	0.0009	0.09317	0.00071	0.9901	0.0075	0.2605	0.0020	0.3577	0.0015
13	2.167	0.010	0.2473	0.0013	2.658	0.017	0.6861	0.0036	0.2049	0.0010	0.09300	0.00050	0.9833	0.0056	0.2581	0.0014	0.3603	0.0015
14	2.173	0.010	0.2450	0.0011	2.650	0.011	0.6936	0.0029	0.2018	0.0008	0.09242	0.00041	0.9950	0.0041	0.2617	0.0011	0.3531	0.0016
15	2.153	0.010	0.2450	0.0011	2.649	0.012	0.6962	0.0033	0.2012	0.0010	0.09249	0.00039	0.9901	0.0041	0.2628	0.0012	0.3519	0.0015
16	2.166	0.011	0.2483	0.0012	2.673	0.012	0.6926	0.0030	0.2035	0.0009	0.09290	0.00047	0.9891	0.0048	0.2591	0.0012	0.3585	0.0018
17	2.155	0.011	0.2455	0.0014	2.652	0.013	0.6926	0.0037	0.2016	0.0009	0.09258	0.00047	0.9899	0.0042	0.2612	0.0012	0.3544	0.0019
18	2.162	0.010	0.2458	0.0017	2.688	0.017	0.6950	0.0045	0.2010	0.0010	0.09145	0.00043	0.9835	0.0047	0.2586	0.0011	0.3536	0.0017
19	2.157	0.011	0.2414	0.0010	2.611	0.013	0.6769	0.0032	0.2004	0.0014	0.09243	0.00046	0.9952	0.0070	0.2593	0.0014	0.3564	0.0018
20	2.164	0.009	0.2434	0.0011	2.656	0.021	0.6883	0.0030	0.2013	0.0008	0.09164	0.00071	0.9854	0.0076	0.2592	0.0020	0.3535	0.0015
21	2.192	0.018	0.2440	0.0015	2.657	0.016	0.6845	0.0040	0.2049	0.0021	0.09184	0.00042	0.9823	0.0077	0.2577	0.0011	0.3563	0.0016
22	2.140	0.009	0.2425	0.0010	2.663	0.012	0.6899	0.0032	0.1969	0.0011	0.09104	0.00042	0.9900	0.0058	0.2591	0.0013	0.3514	0.0017
23	2.167	0.012	0.2433	0.0010	2.649	0.015	0.6905	0.0029	0.2009	0.0011	0.09181	0.00052	0.9903	0.0056	0.2607	0.0015	0.3522	0.0016
24	2.147	0.011	0.2483	0.0012	2.649	0.011	0.6857	0.0029	0.2037	0.0009	0.09372	0.00047	0.9878	0.0043	0.2589	0.0011	0.3619	0.0018
25	2.166	0.012	0.2456	0.0012	2.651	0.017	0.6908	0.0034	0.2036	0.0019	0.09263	0.00063	0.9853	0.0097	0.2606	0.0018	0.3555	0.0020
26	2.150	0.010	0.2501	0.0012	2.663	0.014	0.6936	0.0049	0.2061	0.0013	0.09389	0.00053	0.9797	0.0068	0.2604	0.0020	0.3605	0.0027
27	2.160	0.012	0.2508	0.0014	2.662	0.015	0.6875	0.0034	0.2073	0.0012	0.09417	0.00052	0.9817	0.0056	0.2583	0.0013	0.3645	0.0018
28	2.158	0.010	0.2451	0.0011	2.621	0.011	0.6762	0.0028	0.2034	0.0008	0.09346	0.00042	0.9918	0.0042	0.2580	0.0011	0.3621	0.0016
29	2.145	0.013	0.2466	0.0017	2.655	0.015	0.6836	0.0034	0.2022	0.0009	0.09286	0.00064	0.9854	0.0051	0.2575	0.0013	0.3605	0.0023
30	2.157	0.012	0.2489	0.0011	2.645	0.011	0.6900	0.0027	0.2058	0.0011	0.09408	0.00042	0.9862	0.0041	0.2609	0.0011	0.3605	0.0016
31	2.160	0.014	0.2474	0.0011	2.669	0.012	0.6912	0.0030	0.2035	0.0012	0.09270	0.00044	0.9840	0.0044	0.2590	0.0012	0.3578	0.0017
32	2.171	0.009	0.2486	0.0016	2.679	0.017	0.6935	0.0045	0.2020	0.0009	0.09280	0.00039	0.9977	0.0046	0.2589	0.0011	0.3583	0.0015
33	2.158	0.015	0.2478	0.0013	2.659	0.011	0.6964	0.0032	0.2036	0.0012	0.09317	0.00051	0.9880	0.0046	0.2619	0.0012	0.3558	0.0020
34	2.157	0.016	0.2430	0.0011	2.643	0.013	0.6788	0.0032	0.2011	0.0018	0.09191	0.00045	0.9861	0.0072	0.2569	0.0013	0.3577	0.0017
35	2.196	0.015	0.2432	0.0017	2.659	0.018	0.6974	0.0066	0.2029	0.0015	0.09146	0.00044	0.9899	0.0055	0.2623	0.0021	0.3487	0.0029
36	2.181	0.011	0.2447	0.0012	2.653	0.015	0.6944	0.0030	0.2039	0.0015	0.09222	0.00054	0.9866	0.0078	0.2618	0.0015	0.3523	0.0017
37	2.166	0.015	0.2421	0.0015	2.619	0.013	0.6769	0.0036	0.2013	0.0012	0.09240	0.00055	0.9945	0.0045	0.2585	0.0013	0.3574	0.0022
38	2.150	0.018	0.2480	0.0024	2.647	0.023	0.6868	0.0046	0.2032	0.0009	0.09363	0.00092	0.9906	0.0070	0.2594	0.0018	0.3608	0.0030
39	2.165	0.011	0.2508	0.0013	2.687	0.012	0.7026	0.0031	0.2050	0.0009	0.09334	0.00049	0.9860	0.0045	0.2615	0.0012	0.3569	0.0019
40	2.171	0.012	0.2515	0.0014	2.681	0.015	0.7035	0.0039	0.2057	0.0011	0.09379	0.00044	0.9901	0.0048	0.2624	0.0012	0.3574	0.0017
41	2.164	0.009	0.2450	0.0011	2.647	0.011	0.6855	0.0032	0.2021	0.0010	0.09253	0.00040	0.9911	0.0047	0.2590	0.0012	0.3572	0.0017

42	2.151	0.011	0.2457	0.0011	2.665	0.011	0.6946	0.0035	0.2006	0.0010	0.09220	0.00043	0.9892	0.0045	0.2607	0.0013	0.3537	0.0019
43	2.159	0.016	0.2441	0.0021	2.650	0.017	0.6927	0.0040	0.2004	0.0009	0.09209	0.00074	0.9923	0.0052	0.2614	0.0013	0.3523	0.0026
44	2.187	0.014	0.2455	0.0015	2.651	0.012	0.6939	0.0029	0.2040	0.0009	0.09259	0.00057	0.9926	0.0045	0.2618	0.0012	0.3537	0.0021
45	2.165	0.011	0.2461	0.0011	2.655	0.019	0.6931	0.0030	0.2023	0.0010	0.09269	0.00065	0.9918	0.0070	0.2610	0.0018	0.3551	0.0015
46	2.154	0.012	0.2468	0.0011	2.661	0.011	0.6909	0.0035	0.2040	0.0011	0.09272	0.00041	0.9789	0.0042	0.2596	0.0013	0.3570	0.0019
47	2.165	0.010	0.2441	0.0011	2.645	0.012	0.6798	0.0031	0.2036	0.0009	0.09227	0.00043	0.9813	0.0044	0.2571	0.0012	0.3587	0.0017
48	2.154	0.010	0.2465	0.0011	2.628	0.014	0.6914	0.0051	0.2016	0.0009	0.09374	0.00049	1.0021	0.0052	0.2631	0.0021	0.3563	0.0026
49	2.153	0.014	0.2419	0.0011	2.653	0.022	0.6849	0.0053	0.1973	0.0013	0.09115	0.00074	0.9947	0.0081	0.2582	0.0026	0.3530	0.0027
50	2.143	0.011	0.2471	0.0017	2.675	0.017	0.6870	0.0061	0.2029	0.0010	0.09239	0.00049	0.9758	0.0048	0.2568	0.0020	0.3595	0.0029
51	2.158	0.014	0.2440	0.0011	2.655	0.011	0.6839	0.0035	0.2018	0.0013	0.09188	0.00041	0.9830	0.0043	0.2576	0.0013	0.3565	0.0019
52	2.142	0.015	0.2426	0.0018	2.626	0.019	0.6833	0.0057	0.1996	0.0016	0.09234	0.00043	0.9914	0.0060	0.2602	0.0016	0.3548	0.0022
53	2.153	0.010	0.2440	0.0014	2.656	0.020	0.6818	0.0037	0.2007	0.0010	0.09187	0.00064	0.9854	0.0069	0.2567	0.0017	0.3576	0.0017
54	2.171	0.012	0.2447	0.0012	2.658	0.013	0.6901	0.0038	0.2023	0.0012	0.09206	0.00053	0.9876	0.0064	0.2596	0.0016	0.3545	0.0022
55	2.172	0.010	0.2439	0.0013	2.656	0.014	0.6907	0.0058	0.2016	0.0017	0.09182	0.00043	0.9891	0.0081	0.2601	0.0020	0.3530	0.0028
57	2.171	0.012	0.2474	0.0014	2.684	0.013	0.6987	0.0038	0.2034	0.0017	0.09220	0.00048	0.9840	0.0084	0.2604	0.0014	0.3541	0.0021
58	2.148	0.013	0.2464	0.0013	2.639	0.015	0.6876	0.0037	0.2021	0.0012	0.09332	0.00047	0.9922	0.0049	0.2606	0.0013	0.3581	0.0017
59	2.157	0.015	0.2445	0.0012	2.643	0.013	0.6779	0.0032	0.2025	0.0014	0.09246	0.00046	0.9850	0.0050	0.2565	0.0013	0.3602	0.0017
60	2.170	0.010	0.2447	0.0011	2.645	0.014	0.6854	0.0034	0.2018	0.0009	0.09249	0.00048	0.9946	0.0050	0.2592	0.0014	0.3568	0.0018
61	2.157	0.014	0.2409	0.0018	2.659	0.016	0.6889	0.0062	0.1988	0.0014	0.09059	0.00056	0.9830	0.0069	0.2591	0.0021	0.3496	0.0032
62	2.149	0.018	0.2404	0.0011	2.664	0.016	0.6836	0.0029	0.1981	0.0016	0.09024	0.00055	0.9788	0.0058	0.2566	0.0015	0.3515	0.0016
63	2.170	0.011	0.2429	0.0020	2.637	0.032	0.6874	0.0057	0.2025	0.0010	0.09208	0.00091	0.9870	0.0097	0.2607	0.0026	0.3533	0.0016
64	2.165	0.021	0.2448	0.0015	2.656	0.013	0.6805	0.0034	0.2034	0.0018	0.09218	0.00059	0.9808	0.0048	0.2563	0.0013	0.3594	0.0023
65	2.171	0.012	0.2468	0.0013	2.626	0.016	0.6853	0.0033	0.2069	0.0009	0.09390	0.00066	0.9854	0.0062	0.2610	0.0017	0.3598	0.0021
66	2.171	0.014	0.2459	0.0012	2.662	0.012	0.6925	0.0035	0.2034	0.0012	0.09238	0.00046	0.9862	0.0046	0.2602	0.0014	0.3550	0.0020
67	2.162	0.011	0.2504	0.0012	2.687	0.018	0.6969	0.0030	0.2048	0.0012	0.09318	0.00066	0.9837	0.0073	0.2593	0.0017	0.3592	0.0018
68	2.173	0.018	0.2474	0.0020	2.646	0.013	0.6933	0.0030	0.2049	0.0011	0.09346	0.00077	0.9914	0.0055	0.2620	0.0013	0.3568	0.0028
69	2.164	0.013	0.2480	0.0017	2.665	0.016	0.6946	0.0041	0.2044	0.0010	0.09304	0.00055	0.9849	0.0045	0.2606	0.0012	0.3570	0.0021
70	2.172	0.016	0.2422	0.0017	2.636	0.012	0.6831	0.0030	0.2018	0.0009	0.09184	0.00067	0.9883	0.0047	0.2592	0.0012	0.3543	0.0025
71	2.158	0.012	0.2451	0.0013	2.657	0.014	0.6954	0.0037	0.2026	0.0026	0.09225	0.00043	0.9825	0.0121	0.2617	0.0012	0.3526	0.0017
72	2.162	0.012	0.2500	0.0013	2.655	0.016	0.6980	0.0031	0.2040	0.0010	0.09413	0.00062	0.9984	0.0061	0.2629	0.0016	0.3582	0.0018
74	2.149	0.012	0.2478	0.0012	2.664	0.012	0.6916	0.0030	0.2022	0.0010	0.09300	0.00046	0.9890	0.0045	0.2596	0.0012	0.3581	0.0017
75	2.170	0.012	0.2480	0.0013	2.672	0.014	0.6916	0.0038	0.2029	0.0012	0.09284	0.00043	0.9934	0.0050	0.2588	0.0013	0.3586	0.0018
76	2.145	0.010	0.2490	0.0011	2.665	0.011	0.6971	0.0052	0.2028	0.0013	0.09343	0.00042	0.9890	0.0058	0.2616	0.0020	0.3572	0.0027
77	2.165	0.010	0.2483	0.0012	2.660	0.014	0.7024	0.0035	0.2041	0.0010	0.09334	0.00052	0.9905	0.0054	0.2640	0.0015	0.3538	0.0019
78	2.176	0.010	0.2475	0.0013	2.637	0.013	0.6902	0.0039	0.2068	0.0009	0.09382	0.00043	0.9868	0.0044	0.2618	0.0013	0.3585	0.0019
79	2.150	0.013	0.2510	0.0011	2.659	0.019	0.6990	0.0030	0.2048	0.0013	0.09437	0.00068	0.9911	0.0071	0.2628	0.0019	0.3592	0.0016
80	2.159	0.014	0.2465	0.0014	2.678	0.012	0.6917	0.0053	0.2010	0.0011	0.09205	0.00055	0.9889	0.0046	0.2583	0.0020	0.3563	0.0030
81	2.156	0.011	0.2455	0.0018	2.653	0.020	0.6910	0.0051	0.2026	0.0013	0.09254	0.00047	0.9849	0.0049	0.2605	0.0013	0.3553	0.0016
82	2.177	0.011	0.2429	0.0012	2.640	0.012	0.6875	0.0050	0.2016	0.0009	0.09200	0.00046	0.9934	0.0045	0.2605	0.0019	0.3533	0.0027
83	2.169	0.011	0.2423	0.0012	2.634	0.012	0.6705	0.0031	0.2028	0.0017	0.09197	0.00042	0.9838	0.0079	0.2547	0.0011	0.3606	0.0017
84	2.168	0.011	0.2494	0.0017	2.696	0.017	0.7105	0.0052	0.2037	0.0009	0.09257	0.00048	0.9849	0.0045	0.2635	0.0016	0.3516	0.0022
85	2.158	0.011	0.2495	0.0012	2.674	0.013	0.7052	0.0033	0.2050	0.0014	0.09332	0.00044	0.9828	0.0063	0.2636	0.0012	0.3542	0.0016
86	2.158	0.017	0.2484	0.0019	2.689	0.017	0.6944	0.0030	0.2032	0.0012	0.09243	0.00084	0.9816	0.0074	0.2582	0.0016	0.3578	0.0028
87	2.164	0.017	0.2468	0.0020	2.659	0.013	0.6886	0.0034	0.2039	0.0010	0.09282	0.00070	0.9851	0.0046	0.2590	0.0012	0.3583	0.0027
89	2.188	0.018	0.2436	0.0019	2.650	0.017	0.6869	0.0032	0.2048	0.0011	0.09195	0.00080	0.9820	0.0061	0.2593	0.0016	0.3546	0.0027

Table 3 (*continued*)

Analysis number	$^{208}Pb/^{206}Pb$	$\pm^{208}Pb/^{206}Pb$	$^{206}Pb/^{238}U$	$\pm^{206}Pb/^{238}U$	$^{254}U/^{238}U$	$\pm^{254}U/^{238}U$	$^{270}U/^{238}U$	$\pm^{270}U/^{238}U$	$^{208}Pb/^{248}Th$	$\pm^{208}Pb/^{248}Th$	$^{206}Pb/^{254}U$	$\pm^{206}Pb/^{254}U$	$^{248}Th/^{254}U$	$\pm^{248}Th/^{254}U$	$^{270}U/^{254}U$	$\pm^{270}U/^{254}U$	$^{206}Pb/^{270}U$	$\pm^{206}Pb/^{270}U$
90	2.158	0.012	0.2472	0.0014	2.646	0.021	0.6861	0.0034	0.2041	0.0009	0.09340	0.00075	0.9878	0.0074	0.2593	0.0019	0.3601	0.0019
91	2.179	0.011	0.2425	0.0012	2.641	0.014	0.6847	0.0042	0.2018	0.0011	0.09181	0.00050	0.9917	0.0056	0.2593	0.0017	0.3541	0.0022
92	2.164	0.017	0.2462	0.0012	2.667	0.014	0.6897	0.0031	0.2045	0.0017	0.09236	0.00053	0.9769	0.0059	0.2586	0.0014	0.3570	0.0018
93	2.151	0.014	0.2494	0.0016	2.654	0.018	0.6902	0.0031	0.2040	0.0010	0.09396	0.00077	0.9914	0.0070	0.2601	0.0018	0.3612	0.0023
94	2.159	0.011	0.2490	0.0012	2.650	0.012	0.6883	0.0030	0.2053	0.0015	0.09393	0.00046	0.9882	0.0072	0.2597	0.0012	0.3616	0.0017
95	2.163	0.012	0.2464	0.0013	2.638	0.020	0.6807	0.0036	0.2052	0.0010	0.09337	0.00077	0.9846	0.0076	0.2581	0.0021	0.3616	0.0023
97	2.169	0.012	0.2477	0.0012	2.657	0.013	0.6903	0.0033	0.2047	0.0011	0.09320	0.00044	0.9875	0.0044	0.2598	0.0011	0.3588	0.0017
101	2.175	0.011	0.2454	0.0012	2.678	0.012	0.6896	0.0028	0.2037	0.0009	0.09164	0.00046	0.9785	0.0043	0.2575	0.0011	0.3558	0.0017
102	2.160	0.017	0.2465	0.0013	2.639	0.014	0.6880	0.0035	0.2034	0.0016	0.09339	0.00041	0.9922	0.0043	0.2607	0.0011	0.3583	0.0015
103	2.150	0.009	0.2434	0.0013	2.649	0.014	0.6823	0.0037	0.2002	0.0009	0.09188	0.00040	0.9869	0.0044	0.2575	0.0011	0.3568	0.0015
104	2.161	0.015	0.2458	0.0017	2.653	0.011	0.6794	0.0030	0.2034	0.0009	0.09267	0.00063	0.9845	0.0042	0.2561	0.0011	0.3618	0.0025
105	2.148	0.009	0.2459	0.0013	2.655	0.014	0.6879	0.0036	0.2011	0.0010	0.09261	0.00040	0.9889	0.0047	0.2591	0.0011	0.3574	0.0016
106	2.160	0.013	0.2442	0.0018	2.655	0.020	0.6854	0.0051	0.2015	0.0011	0.09195	0.00040	0.9853	0.0042	0.2581	0.0011	0.3562	0.0016
107	2.168	0.013	0.2477	0.0013	2.663	0.012	0.7061	0.0030	0.2042	0.0011	0.09302	0.00051	0.9875	0.0046	0.2652	0.0012	0.3508	0.0018
108	2.173	0.009	0.2452	0.0010	2.669	0.013	0.7042	0.0030	0.2013	0.0009	0.09188	0.00047	0.9916	0.0050	0.2639	0.0014	0.3482	0.0016
109	2.163	0.011	0.2415	0.0012	2.648	0.011	0.6918	0.0033	0.1992	0.0010	0.09120	0.00045	0.9904	0.0050	0.2613	0.0013	0.3491	0.0019
110	2.174	0.011	0.2451	0.0014	2.662	0.014	0.6908	0.0037	0.2024	0.0016	0.09206	0.00043	0.9887	0.0074	0.2595	0.0011	0.3548	0.0016
111	2.165	0.017	0.2379	0.0018	2.661	0.011	0.6847	0.0052	0.1965	0.0009	0.08939	0.00069	0.9846	0.0042	0.2574	0.0020	0.3474	0.0035
112	2.176	0.010	0.2411	0.0011	2.708	0.013	0.6948	0.0066	0.2003	0.0008	0.08904	0.00045	0.9676	0.0045	0.2566	0.0025	0.3470	0.0033
113	2.154	0.014	0.2379	0.0020	2.642	0.018	0.6766	0.0046	0.1959	0.0008	0.09005	0.00059	0.9902	0.0042	0.2561	0.0011	0.3517	0.0023
114	2.172	0.009	0.2402	0.0010	2.637	0.011	0.6774	0.0029	0.2002	0.0013	0.09109	0.00041	0.9883	0.0063	0.2569	0.0012	0.3546	0.0016
115	2.175	0.015	0.2409	0.0010	2.679	0.011	0.6895	0.0029	0.1992	0.0015	0.08989	0.00039	0.9814	0.0048	0.2573	0.0011	0.3493	0.0016
116	2.143	0.013	0.2492	0.0012	2.690	0.014	0.7077	0.0035	0.2005	0.0013	0.09264	0.00047	0.9901	0.0053	0.2631	0.0014	0.3522	0.0017
117	2.170	0.011	0.2408	0.0010	2.645	0.020	0.6837	0.0028	0.1986	0.0014	0.09105	0.00068	0.9947	0.0089	0.2585	0.0019	0.3522	0.0015
118	2.145	0.012	0.2497	0.0016	2.697	0.026	0.7028	0.0050	0.2027	0.0011	0.09259	0.00078	0.9797	0.0083	0.2606	0.0023	0.3553	0.0019
119	2.156	0.013	0.2430	0.0012	2.645	0.011	0.6825	0.0028	0.2010	0.0010	0.09190	0.00046	0.9857	0.0042	0.2581	0.0011	0.3561	0.0018
120	2.173	0.012	0.2448	0.0011	2.656	0.011	0.6886	0.0032	0.2023	0.0011	0.09218	0.00042	0.9899	0.0045	0.2593	0.0012	0.3555	0.0018
121	2.152	0.012	0.2409	0.0016	2.618	0.018	0.6712	0.0040	0.1997	0.0008	0.09200	0.00062	0.9915	0.0056	0.2564	0.0016	0.3589	0.0022
122	2.168	0.010	0.2432	0.0013	2.687	0.021	0.7026	0.0047	0.2004	0.0014	0.09051	0.00069	0.9789	0.0091	0.2614	0.0023	0.3462	0.0022
123	2.165	0.009	0.2463	0.0013	2.668	0.014	0.6995	0.0038	0.2024	0.0009	0.09232	0.00040	0.9872	0.0042	0.2622	0.0012	0.3521	0.0016
124	2.159	0.019	0.2491	0.0018	2.712	0.016	0.6995	0.0030	0.2023	0.0013	0.09185	0.00078	0.9803	0.0061	0.2579	0.0016	0.3561	0.0026
125	2.167	0.012	0.2430	0.0020	2.627	0.020	0.6920	0.0059	0.2010	0.0009	0.09248	0.00052	0.9971	0.0046	0.2634	0.0017	0.3511	0.0024
126	2.171	0.013	0.2488	0.0012	2.657	0.020	0.6952	0.0030	0.2060	0.0014	0.09364	0.00073	0.9867	0.0083	0.2617	0.0020	0.3578	0.0017
127	2.162	0.010	0.2507	0.0011	2.653	0.011	0.6965	0.0033	0.2070	0.0010	0.09447	0.00043	0.9867	0.0049	0.2625	0.0013	0.3599	0.0018
128	2.159	0.011	0.2490	0.0013	2.681	0.012	0.7058	0.0051	0.2038	0.0011	0.09289	0.00049	0.9841	0.0054	0.2633	0.0019	0.3528	0.0027
129	2.184	0.017	0.2467	0.0017	2.624	0.013	0.6870	0.0032	0.2063	0.0015	0.09402	0.00063	0.9957	0.0056	0.2618	0.0012	0.3591	0.0024

130	2.155	0.018	0.2460	0.0011	2.604	0.012	0.6763	0.0030	0.2050	0.0018	0.09448	0.00045	0.9935	0.0059	0.2598	0.0012	0.3637	0.0016
131	2.174	0.014	0.2475	0.0016	2.676	0.012	0.6905	0.0033	0.2049	0.0010	0.09249	0.00058	0.9812	0.0046	0.2580	0.0012	0.3585	0.0023
132	2.179	0.011	0.2501	0.0013	2.661	0.016	0.7019	0.0035	0.2071	0.0016	0.09398	0.00054	0.9887	0.0079	0.2637	0.0015	0.3563	0.0017
133	2.156	0.018	0.2500	0.0011	2.640	0.015	0.6877	0.0033	0.2044	0.0018	0.09470	0.00055	0.9987	0.0068	0.2605	0.0016	0.3635	0.0018
134	2.134	0.012	0.2491	0.0014	2.683	0.018	0.6995	0.0042	0.2012	0.0009	0.09285	0.00068	0.9844	0.0065	0.2608	0.0020	0.3561	0.0023
135	2.144	0.014	0.2505	0.0016	2.681	0.012	0.7005	0.0031	0.2037	0.0009	0.09346	0.00061	0.9839	0.0045	0.2613	0.0012	0.3576	0.0023
136	2.160	0.015	0.2447	0.0015	2.665	0.016	0.6933	0.0038	0.2008	0.0013	0.09179	0.00054	0.9873	0.0051	0.2601	0.0013	0.3529	0.0019
137	2.173	0.011	0.2502	0.0013	2.701	0.017	0.7024	0.0036	0.2045	0.0009	0.09262	0.00059	0.9844	0.0061	0.2600	0.0016	0.3562	0.0018
138	2.163	0.010	0.2472	0.0014	2.657	0.015	0.6949	0.0037	0.2029	0.0014	0.09302	0.00048	0.9916	0.0071	0.2615	0.0013	0.3557	0.0017
139	2.157	0.015	0.2442	0.0017	2.628	0.013	0.6907	0.0033	0.2002	0.0009	0.09291	0.00067	1.0012	0.0050	0.2628	0.0014	0.3536	0.0025
140	2.171	0.017	0.2379	0.0017	2.633	0.011	0.6788	0.0029	0.1987	0.0012	0.09035	0.00066	0.9874	0.0051	0.2578	0.0011	0.3505	0.0026
141	2.162	0.009	0.2434	0.0013	2.629	0.015	0.6749	0.0035	0.2014	0.0008	0.09258	0.00043	0.9940	0.0045	0.2567	0.0012	0.3607	0.0015
142	2.147	0.013	0.2435	0.0012	2.640	0.011	0.6886	0.0049	0.2004	0.0012	0.09225	0.00047	0.9882	0.0049	0.2608	0.0019	0.3537	0.0027
143	2.149	0.009	0.2465	0.0014	2.635	0.014	0.6916	0.0041	0.2010	0.0009	0.09353	0.00041	0.9998	0.0043	0.2625	0.0013	0.3564	0.0018
144	2.169	0.010	0.2394	0.0011	2.644	0.019	0.6793	0.0055	0.1974	0.0011	0.09054	0.00066	0.9947	0.0079	0.2569	0.0025	0.3524	0.0029
145	2.154	0.010	0.2434	0.0011	2.678	0.011	0.6955	0.0029	0.1988	0.0010	0.09089	0.00042	0.9853	0.0051	0.2598	0.0011	0.3499	0.0016
146	2.168	0.019	0.2380	0.0012	2.656	0.011	0.6884	0.0032	0.1978	0.0017	0.08960	0.00046	0.9821	0.0050	0.2592	0.0012	0.3457	0.0019
147	2.154	0.013	0.2473	0.0012	2.659	0.013	0.6906	0.0033	0.2029	0.0015	0.09302	0.00041	0.9875	0.0062	0.2598	0.0011	0.3581	0.0016
148	2.153	0.012	0.2427	0.0011	2.640	0.014	0.6886	0.0029	0.1998	0.0012	0.09195	0.00049	0.9911	0.0061	0.2609	0.0014	0.3525	0.0016
149	2.157	0.010	0.2422	0.0012	2.659	0.013	0.6886	0.0040	0.1988	0.0009	0.09108	0.00041	0.9882	0.0045	0.2590	0.0015	0.3517	0.0020
150	2.167	0.016	0.2427	0.0017	2.643	0.016	0.6947	0.0038	0.2007	0.0012	0.09184	0.00059	0.9912	0.0048	0.2629	0.0013	0.3494	0.0021
Average	2.163		0.2457		2.656		0.6903		0.2026		0.09250		0.9875		0.2599		0.3559	
Standard deviation	0.011		0.0031		0.019		0.0076		0.0025		0.00113		0.0055		0.0020		0.0040	
Standard deviation (%)	0.52		1.27		0.73		1.10		1.22		1.22		0.56		0.79		1.12	
Standard error	0.00094		0.00026		0.00162		0.00064		0.00021		0.00009		0.00046		0.00017		0.00033	
Standard error (%)	0.04		0.11		0.06		0.09		0.10		0.10		0.05		0.07		0.09	
Skew	0.21		− 0.32		0.21		0.01		− 0.02		− 0.42		− 0.19		0.03		− 0.14	
Kurtosis	0.19		− 0.37		0.35		0.10		0.51		0.53		0.94		− 0.50		− 0.18	
Avg. error (%)	0.58		0.55		0.55		0.54		0.58		0.58		0.58		0.56		0.56	

ratios approximate a normally distributed population requires that a sufficiently large number of accurate ion probe measurements should be able to duplicate this 'limiting' distribution.

The TIMS U–Th–Pb data for eight fragments of SRM 610 glass having approximate masses of $3-12$ µg are presented in Table 2. Elemental abundances are not reported because the fragments were small and their weighing uncertainties relatively large. The $^{238}U/^{235}U$ ratio was determined from this study to be 417.8, which is similar to the value of 419.9 given by Reed (1992). The $^{206}Pb/^{238}U$ values are indistinguishable within analytical error, having a weighted mean of 0.25664 ± 0.00022 (2σ; MSWD = 0.57, probability of fit, $P=0.78$). This compares well with the value of 0.2569 calculated from published isotopic and elemental compositions (see above). There is no evidence in the TIMS data for heterogeneity in the $^{206}Pb/^{238}U$ values. The weighted mean $^{206}Pb/^{204}Pb$, $^{207}Pb/^{204}Pb$, and $^{208}Pb/^{204}Pb$ are 17.0436 ± 0.0077, 15.4995 ± 0.0076, and 36.959 ± 0.024, slightly lower but within error of the values proposed by Woodhead and Hergt (2001). The mean TIMS $^{208}Pb/^{206}Pb$ of 2.1685 ± 0.0018 is within error of the reference value of 2.1690 ± 0.0001. The mean TIMS Th/U and Th/Pb (wt.) are 0.9866 ± 0.0018 (2σ; MSWD = 0.69, $P=0.68$) and 1.0706 ± 0.0022 (2σ; MSWD = 1.2, $P=0.28$), respectively, which are identical within error to the values of 0.9867 and 1.069 reported by Rocholl et al. (2000).

5.2. SIMS U–Pb results for SRM 610

A total of 143 spot analyses from the single fragment of SRM 610 glass are presented in Table 3. These data were collected to assess the adequacy of within-spot and within-session error estimates and to provide a comparison with similar analyses of z6266 zircon (see below). As argued above, the glass can be considered chemically and isotopically homogeneous, especially within a restricted area on a single fragment. Consequently, replicate measurements of $^{208}Pb/^{206}Pb$, Th/U, and Pb/U obtained from multiple spot locations should agree within their analytical errors, i.e., have an MSWD close to 1.

5.2.1. Pb-isotopes

The weighted mean of 143 separate spot measurements of raw $^{208}Pb^+/^{206}Pb^+$ is 2.1623 ± 0.0019 (2σ),

with a MSWD of 0.87 ($P=0.87$), calculated using the within-spot errors. Relative to the accepted value of 2.1690, the mean $^{208}Pb^+/^{206}Pb^+$ indicates isotopic fractionation of 0.15%/amu in favour of the light isotope. The mean individual within-spot error is 0.58% (1σ), just slightly greater than the standard deviation (S) of 0.52% for the data set. As expected for a homogeneous target and reasonable analytical errors, the probability density distribution displays a Gaussian form (Fig. 4a). The results unequivocally demonstrate that the within-spot errors are adequate to explain the data distribution, and are perhaps even slightly overestimated.

5.2.2. Th–U isotopes

The 143 raw $^{248}[ThO]^+/^{254}[UO]^+$ values have $S=$ 0.52%, the mean individual within-spot error is 0.58%, the weighted mean is 0.98638 ± 0.00095 (2σ), and the MSWD is 1.18 (probability = 0.066) calculated using the within-spot errors. The within-spot errors are just barely adequate to explain the scatter. However, the $^{248}[ThO]^+/^{254}[UO]^+$ values are negatively correlated ($R=-0.578$, linear least-squares fit) with $^{254}[UO]^+/^{238}U^+$, allowing them to be corrected to the mean $^{254}[UO]^+/^{238}U^+$ ratio of 2.656. The dispersion of $^{254}[UO]^+/^{238}U^+$ values, although small ($S=0.73\%$), is well outside within-spot errors (MSWD = 1.9, $P=0$). The variable-discriminated-corrected $^{248}[ThO]^+/^{254}[UO]^+$ ($=\{^{248}[ThO]^+/^{254}[UO]^+\}_{UO/O}$) have a weighted mean of 0.98769 ± 0.00087 (2σ), with a MSWD of 0.72 (probability = 0.992), again only using the within-spot errors. The standard deviation of the corrected data is 0.42%, and the distribution appears Gaussian (Fig. 4b). The results show that, following appropriate correction for systematic isotope discrimination, there are no detectable variations in Th/U within the chip of glass, and that the individual within-spot errors are entirely adequate to explain the scatter of data. It is also notable that the mean $^{248}[ThO]^+/^{254}[UO]^+$ and $\{^{248}[ThO]^+/^{254}[UO]^+\}_{UO/O}$ values are practically identical to the accepted Th/U value of 0.987, indicating no significant elemental discrimination.

5.2.3. U–Pb isotopes

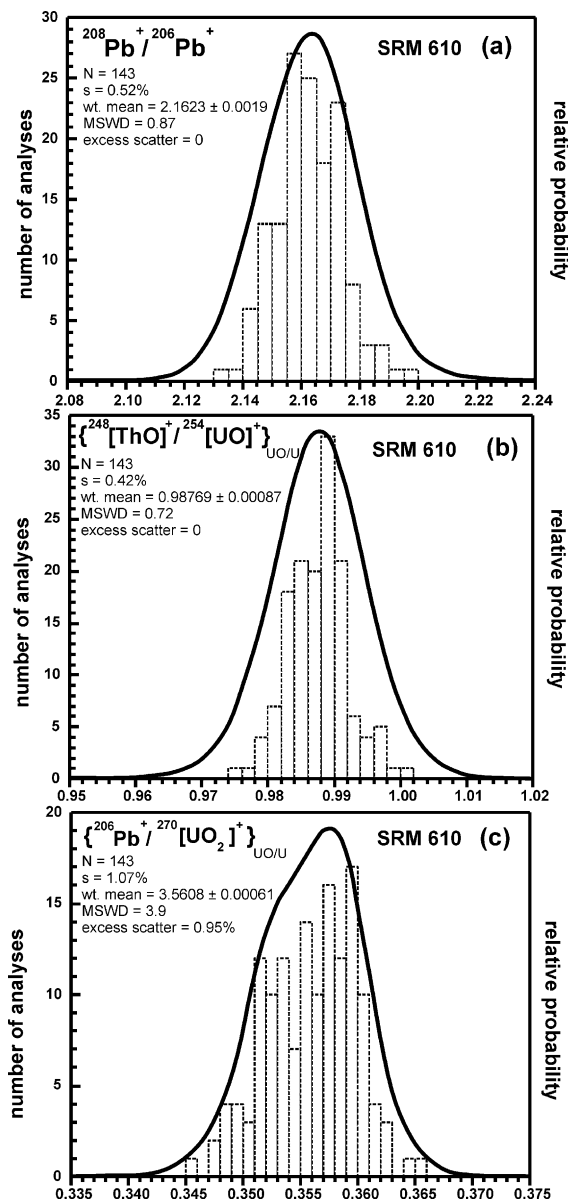All data for $^{206}Pb^+/^{238}U[O_x]^+$ species are similar in showing weak or absent correlations with $^{254}[UO]^+/$

Fig. 4. Probability density distributions and histograms of 143 spot analyses of a fragment of NIST SRM 610 obtained from mount IP109. (a) $^{208}Pb^+/^{206}Pb^+$; (b) $^{248}[ThO]^+/^{254}[UO]^+$ corrected to the mean $^{254}[UO]^+/^{238}U^+$ (see text for details); (c) $^{206}Pb^+/^{270}[UO_2]^+$ values corrected to the mean $^{254}[UO]^+/^{238}U^+$. Note the Gaussian distributions and lack of excess scatter for (a) and (b), in contrast to (c). Abbreviations: N = number of spots, s = standard deviation, MSWD = mean square of weighted deviates.

$^{238}U^+$, and similar dispersion. The mean $^{206}Pb^+/^{238}U^+$ of 0.2457 (Table 3) is 4% lower than the TIMS value of 0.2566. This relationship contrasts with that observed for zircon, where $^{206}Pb^+/^{238}U^+$ is several times *higher* than actual values (see below).

In the following discussion, only the $^{206}Pb^+/^{270}[UO_2]^+$ ratio is considered, as this is the variable used in subsequent analysis of zircon data (see below). The $^{206}Pb^+/^{270}[UO_2]^+$ values show minor systematic variations in elemental discrimination when assessed using the traditional species, e.g., $^{254}[UO]^+/^{238}U^+$. A weak negative linear correlation with $^{254}[UO]^+/^{238}U^+$ ($R = -0.279$) is observed, and the data were accordingly corrected to the mean $^{254}[UO]^+/^{238}U^+$, i.e., $\{^{206}Pb^+/^{270}[UO_2]^+\}_{UO/U}$, but the results are indistinguishable from that achieved using the uncorrected values. No significant secondary ion steering differences existed between spot analyses, nor were there any other obvious patterns of $^{206}Pb^+/^{270}[UO_2]^+$ discrimination.

The average within-spot error of individual $\{^{206}Pb^+/^{270}[UO_2]^+\}_{UO/U}$ values is 0.56% (1σ), about half that of the standard deviation ($S = 1.07\%$). Using the within-spot errors, the weighted mean $\{^{206}Pb^+/^{270}[UO_2]^+\}_{UO/U}$ is 0.35608 ± 0.00061 (2σ), and the MSWD value is 3.9 ($P = 0$), clearly indicating that the 143 measurements do not belong to a single population. The $\{^{206}Pb^+/^{270}[UO_2]^+\}_{UO/U}$ data have a significant excess scatter (see Section 4.1) of 0.95%. Of further interest is the fact that the probability density distribution for $\{^{206}Pb^+/^{270}[UO_2]^+\}_{UO/U}$ is non-Gaussian and slightly negatively skewed (Fig. 4c). Slightly higher degrees of excess scatter and similar non-Gaussian distributions are also exhibited by $^{206}Pb^+/^{238}U^+$ and $^{206}Pb^+/^{254}[UO]^+$. The significant excess scatter exhibited by the $\{^{206}Pb^+/^{270}[UO_2]^+\}_{UO/U}$ data contrasts with the results for Pb-isotopes and Th/U measurements, which showed no such excess scatter when the within-spot errors are used.

5.3. SIMS U–Pb results for z6266 zircon

The data from experiment IP222.1, comprising 162 spot analyses from 60 fragments of z6266 zircon are presented in Table 4. A further 63 analyses, acquired in experiment IP222.2 after re-polishing, are presented in Table 5. In both experiments, the common Pb

Table 4
Raw SHRIMP isotopic data ($\pm 1\sigma$) for z6266 zircon, experiment IP222.1

Analysis (6266-grain#.spot#)	^{254}U/ ^{196}Zr	$\pm^{254}$U/ ^{196}Zr	^{270}U/ ^{196}Zr	$\pm^{270}$U/ ^{196}Zr	^{204}Pb/ ^{206}Pb	$\pm^{204}$Pb/ ^{206}Pb	^{206}Pb/ ^{238}U	$\pm^{206}$Pb/ ^{238}U	^{254}U/ ^{238}U	$\pm^{254}$U/ ^{238}U	^{270}U/ ^{238}U	$\pm^{270}$U/ ^{238}U	^{206}Pb/ ^{254}U	$\pm^{206}$Pb/ ^{254}U	^{248}Th/ ^{254}U	$\pm^{248}$Th/ ^{254}U	^{270}U/ ^{254}U	$\pm^{270}$U/ ^{254}U	^{206}Pb/ ^{270}U	$\pm^{206}$Pb/ ^{270}U	^{206}Pb*/ ^{270}U	$\pm^{206}$Pb*/ ^{270}U
6266-1.1	6.221	0.047	2.484	0.021	2.31e−05	2.35e−05	0.2933	0.0013	7.054	0.025	2.816	0.016	0.04158	0.00015	0.19610	0.00087	0.3993	0.0020	0.10415	0.00059	0.10407	0.00059
6266-1.2	6.181	0.025	2.447	0.010	1.37e−05	2.10e−05	0.2882	0.0014	6.963	0.030	2.756	0.012	0.04139	0.00017	0.19724	0.00074	0.3958	0.0015	0.10457	0.00044	0.10451	0.00045
6266-2.1	6.186	0.043	2.491	0.017	1.00e−05	1.00e−05	0.2950	0.0017	7.039	0.040	2.834	0.016	0.04191	0.00017	0.19725	0.00079	0.4026	0.0015	0.10411	0.00040	0.10406	0.00040
6266-2.2	6.193	0.033	2.467	0.010	1.06e−06	1.71e−05	0.2879	0.0023	7.001	0.040	2.788	0.013	0.04112	0.00034	0.19796	0.00107	0.3983	0.0020	0.10325	0.00077	0.10322	0.00077
6266-3.1	5.862	0.022	2.318	0.011	2.92e−05	2.06e−05	0.2763	0.0010	6.963	0.022	2.753	0.012	0.03969	0.00014	0.19502	0.00071	0.3954	0.0017	0.10037	0.00048	0.10032	0.00048
6266-3.2	5.878	0.022	2.355	0.011	2.26e−05	1.93e−05	0.2846	0.0012	6.960	0.026	2.788	0.012	0.04089	0.00014	0.19376	0.00068	0.4006	0.0013	0.10206	0.00040	0.10202	0.00040
6266-3.3	5.881	0.034	2.364	0.011	1.75e−06	2.56e−05	0.2941	0.0012	6.974	0.036	2.804	0.011	0.04217	0.00022	0.19542	0.00157	0.4020	0.0021	0.10490	0.00043	0.10490	0.00043
6266-3.4	5.837	0.028	2.338	0.012	3.64e−05	1.81e−05	0.2888	0.0015	6.996	0.030	2.802	0.013	0.04128	0.00024	0.19448	0.00103	0.4005	0.0021	0.10308	0.00063	0.10302	0.00063
6266-4.1	5.888	0.025	2.368	0.010	8.51e−06	1.01e−05	0.3009	0.0015	7.004	0.032	2.817	0.013	0.04296	0.00020	0.19486	0.00081	0.4022	0.0017	0.10682	0.00050	0.10680	0.00050
6266-4.2	5.926	0.023	2.383	0.010	4.62e−05	2.88e−05	0.2972	0.0015	7.044	0.031	2.832	0.015	0.04219	0.00016	0.19634	0.00090	0.4021	0.0016	0.10493	0.00049	0.10485	0.00049
6266-5.1	6.083	0.022	2.460	0.010	1.37e−05	2.26e−05	0.3069	0.0018	7.178	0.035	2.903	0.015	0.04275	0.00017	0.19610	0.00080	0.4044	0.0013	0.10572	0.00048	0.10568	0.00049
6266-5.2	6.095	0.047	2.492	0.020	1.93e−05	2.28e−05	0.3099	0.0012	7.243	0.023	2.962	0.011	0.04279	0.00015	0.19473	0.00073	0.4089	0.0014	0.10463	0.00042	0.10458	0.00042
6266-5.3	6.095	0.030	2.466	0.014	2.29e−05	3.10e−05	0.3068	0.0013	7.068	0.025	2.860	0.014	0.04340	0.00018	0.19616	0.00077	0.4046	0.0019	0.10727	0.00057	0.10721	0.00058
6266-6.1	6.153	0.023	2.511	0.011	3.05e−05	1.56e−05	0.3047	0.0011	7.308	0.022	2.983	0.011	0.04169	0.00014	0.19609	0.00071	0.4081	0.0014	0.10216	0.00041	0.10208	0.00042
6266-6.2	6.149	0.026	2.509	0.015	2.32e−05	2.67e−05	0.3053	0.0012	7.169	0.027	2.925	0.016	0.04259	0.00015	0.19486	0.00076	0.4081	0.0021	0.10437	0.00056	0.10430	0.00056
6266-6.3	6.074	0.023	2.473	0.017	4.37e−05	2.49e−05	0.3153	0.0021	7.283	0.025	2.966	0.019	0.04329	0.00028	0.19471	0.00079	0.4072	0.0025	0.10631	0.00090	0.10622	0.00090
6266-7.1	6.073	0.028	2.480	0.012	4.83e−05	1.94e−05	0.3082	0.0014	7.245	0.022	2.958	0.011	0.04253	0.00018	0.19548	0.00080	0.4083	0.0013	0.10416	0.00048	0.10406	0.00048
6266-7.2	6.100	0.031	2.464	0.017	3.50e−05	4.55e−05	0.3062	0.0014	7.213	0.036	2.913	0.020	0.04245	0.00019	0.19620	0.00113	0.4039	0.0027	0.10510	0.00068	0.10502	0.00069
6266-8.1	6.030	0.022	2.445	0.012	3.38e−06	1.34e−05	0.2997	0.0014	7.244	0.022	2.938	0.011	0.04138	0.00017	0.19409	0.00068	0.4055	0.0013	0.10204	0.00047	0.10203	0.00047
6266-8.2	6.058	0.037	2.466	0.016	2.16e−05	2.21e−05	0.3096	0.0015	7.247	0.023	2.950	0.011	0.04272	0.00020	0.19485	0.00081	0.4071	0.0014	0.10493	0.00055	0.10488	0.00055
6266-8.3	6.126	0.029	2.503	0.014	1.72e−05	3.34e−05	0.3061	0.0016	7.274	0.036	2.973	0.017	0.04207	0.00019	0.19492	0.00084	0.4087	0.0021	0.10295	0.00054	0.10290	0.00054
6266-9.1	5.858	0.032	2.362	0.016	4.17e−05	1.97e−05	0.2963	0.0022	7.123	0.034	2.873	0.017	0.04159	0.00033	0.19321	0.00097	0.4033	0.0027	0.10314	0.00090	0.10307	0.00090
6266-9.2	5.906	0.023	2.365	0.014	1.00e−05	1.00e−05	0.2863	0.0013	6.984	0.026	2.797	0.012	0.04099	0.00016	0.19445	0.00068	0.4005	0.0013	0.10234	0.00044	0.10232	0.00044
6266-9.3	5.820	0.024	2.344	0.011	7.18e−06	1.04e−05	0.2896	0.0011	7.067	0.022	2.847	0.011	0.04099	0.00014	0.19507	0.00070	0.4029	0.0013	0.10174	0.00041	0.10173	0.00041
6266-10.1	6.094	0.023	2.468	0.011	1.77e−07	1.28e−05	0.3081	0.0018	7.247	0.025	2.935	0.012	0.04252	0.00024	0.19427	0.00088	0.4050	0.0014	0.10497	0.00062	0.10496	0.00062
6266-10.2	6.003	0.024	2.403	0.012	3.40e−05	1.95e−05	0.3070	0.0012	7.096	0.022	2.841	0.012	0.04326	0.00016	0.19419	0.00140	0.4004	0.0016	0.10805	0.00049	0.10799	0.00049
6266-10.3	6.045	0.025	2.434	0.010	1.00e−05	1.00e−05	0.3022	0.0012	7.172	0.023	2.888	0.014	0.04213	0.00014	0.19530	0.00122	0.4026	0.0014	0.10463	0.00045	0.10463	0.00045
6266-11.1	6.003	0.022	2.452	0.010	2.84e−05	1.83e−05	0.3062	0.0019	7.195	0.041	2.938	0.018	0.04256	0.00014	0.19597	0.00084	0.4084	0.0013	0.10420	0.00040	0.10415	0.00041
6266-11.2	6.007	0.029	2.445	0.011	1.84e−05	1.23e−05	0.3094	0.0012	7.230	0.030	2.943	0.011	0.04280	0.00019	0.19445	0.00137	0.4070	0.0017	0.10514	0.00041	0.10511	0.00041
6266-11.3	5.922	0.031	2.406	0.014	6.58e−05	6.07e−05	0.3013	0.0013	7.107	0.030	2.887	0.014	0.04240	0.00019	0.19592	0.00155	0.4063	0.0020	0.10436	0.00051	0.10424	0.00052
6266-12.1	6.104	0.024	2.478	0.013	2.00e−05	2.95e−05	0.3022	0.0012	7.238	0.022	2.938	0.014	0.04176	0.00019	0.19584	0.00066	0.4059	0.0018	0.10288	0.00054	0.10283	0.00054
6266-12.2	6.121	0.026	2.499	0.011	3.00e−05	1.94e−05	0.3156	0.0013	7.236	0.024	2.954	0.011	0.04362	0.00016	0.19535	0.00074	0.4082	0.0013	0.10684	0.00044	0.10677	0.00044
6266-12.3	6.138	0.032	2.511	0.012	6.12e−06	1.77e−05	0.3036	0.0015	7.239	0.030	2.961	0.011	0.04194	0.00023	0.19757	0.00098	0.4091	0.0018	0.10252	0.00053	0.10249	0.00053
6266-13.1	6.211	0.024	2.518	0.012	5.33e−05	4.41e−05	0.3009	0.0018	7.208	0.040	2.922	0.018	0.04174	0.00014	0.19688	0.00066	0.4054	0.0015	0.10296	0.00044	0.10283	0.00044
6266-13.2	6.223	0.045	2.546	0.022	1.00e−05	1.00e−05	0.3090	0.0018	7.248	0.039	2.966	0.021	0.04264	0.00029	0.19509	0.00107	0.4092	0.0032	0.10420	0.00085	0.10414	0.00085
6266-14.1	6.109	0.027	2.481	0.010	1.00e−05	1.00e−05	0.3015	0.0015	7.329	0.030	2.976	0.011	0.04114	0.00020	0.19542	0.00087	0.4060	0.0016	0.10133	0.00051	0.10130	0.00051
6266-14.2	6.084	0.023	2.476	0.012	2.44e−06	2.66e−05	0.3150	0.0015	7.216	0.030	2.936	0.015	0.04366	0.00016	0.19725	0.00070	0.4069	0.0016	0.10729	0.00051	0.10727	0.00052
6266-15.1	6.129	0.027	2.486	0.013	1.00e−05	1.00e−05	0.3038	0.0011	7.229	0.028	2.932	0.015	0.04203	0.00018	0.19615	0.00122	0.4056	0.0022	0.10362	0.00055	0.10358	0.00055
6266-15.2	6.161	0.025	2.508	0.012	1.16e−05	2.08e−05	0.3019	0.0015	7.198	0.031	2.931	0.014	0.04194	0.00015	0.19510	0.00068	0.4071	0.0014	0.10301	0.00043	0.10296	0.00043
6266-16.2	5.923	0.030	2.421	0.012	5.50e−06	7.64e−06	0.3087	0.0016	7.173	0.032	2.932	0.011	0.04304	0.00025	0.19623	0.00125	0.4088	0.0019	0.10528	0.00055	0.10527	0.00055
6266-17.1	5.826	0.028	2.336	0.012	4.84e−05	3.24e−05	0.2970	0.0012	6.996	0.028	2.804	0.012	0.04246	0.00016	0.19525	0.00097	0.4009	0.0016	0.10591	0.00044	0.10582	0.00044
6266-17.2	5.804	0.022	2.352	0.013	1.00e−05	1.00e−05	0.3005	0.0018	7.052	0.030	2.858	0.017	0.04262	0.00021	0.19401	0.00071	0.4053	0.0020	0.10515	0.00067	0.10513	0.00067
6266-18.1	6.247	0.043	2.544	0.018	2.22e−05	2.14e−05	0.3017	0.0018	7.226	0.034	2.942	0.014	0.04175	0.00024	0.19448	0.00109	0.4072	0.0018	0.10254	0.00060	0.10246	0.00060
6266-18.2	6.191	0.023	2.505	0.014	4.40e−05	2.54e−05	0.3125	0.0013	7.229	0.029	2.926	0.011	0.04323	0.00016	0.19663	0.00089	0.4047	0.0020	0.10682	0.00058	0.10671	0.00058
6266-18.3	6.230	0.024	2.522	0.014	7.64e−05	4.20e−05	0.3142	0.0024	7.207	0.025	2.917	0.016	0.04361	0.00032	0.19461	0.00070	0.4048	0.0020	0.10772	0.00092	0.10754	0.00093
6266-19.1	5.923	0.023	2.396	0.010	1.44e−05	1.70e−05	0.3042	0.0017	7.268	0.024	2.940	0.011	0.04185	0.00023	0.19210	0.00133	0.4045	0.0014	0.10346	0.00059	0.10343	0.00059
6266-19.2	5.857	0.022	2.375	0.010	5.57e−06	7.85e−06	0.3069	0.0012	7.218	0.024	2.927	0.011	0.04252	0.00015	0.19423	0.00075	0.4055	0.0013	0.10485	0.00041	0.10484	0.00041
6266-19.3	5.908	0.028	2.421	0.014	4.01e−05	7.04e−05	0.3142	0.0019	7.296	0.032	2.990	0.017	0.04306	0.00027	0.19160	0.00087	0.4098	0.0024	0.10509	0.00076	0.10502	0.00077
6266-20.1	6.148	0.030	2.512	0.015	1.27e−05	2.15e−05	0.3102	0.0015	7.307	0.036	2.986	0.018	0.04245	0.00019	0.19428	0.00103	0.4086	0.0023	0.10388	0.00057	0.10383	0.00057
6266-20.2	6.102	0.024	2.491	0.011	5.33e−05	2.34e−05	0.3104	0.0015	7.280	0.031	2.972	0.014	0.04264	0.00016	0.19452	0.00082	0.4083	0.0015	0.10445	0.00045	0.10434	0.00045
6266-20.3	6.119	0.027	2.512	0.011	1.00e−05	1.00e−05	0.3216	0.0022	7.386	0.029	3.032	0.012	0.04355	0.00030	0.19421	0.00080	0.4104	0.0016	0.10610	0.00074	0.10606	0.00074

6266-21.1	5.966	0.029	2.442	0.013	1.09e−05	9.40e−06	0.3109	0.0015	7.309	0.030	2.991	0.013	0.04254	0.00016	0.19246	0.00070	0.4092	0.0014	0.10395	0.00043	0.10393	0.00043
6266-21.2	5.923	0.049	2.422	0.021	1.40e−05	1.99e−05	0.3116	0.0021	7.296	0.046	2.983	0.020	0.04271	0.00015	0.19346	0.00070	0.4089	0.0014	0.10446	0.00044	0.10443	0.00044
6266-21.3	5.928	0.029	2.415	0.010	1.48e−05	1.55e−05	0.3004	0.0013	7.225	0.035	2.944	0.012	0.04158	0.00015	0.19319	0.00152	0.4075	0.0019	0.10204	0.00042	0.10201	0.00042
6266-22.1	5.930	0.022	2.430	0.010	4.64e−05	2.81e−05	0.3122	0.0012	7.253	0.022	2.972	0.011	0.04305	0.00014	0.19624	0.00080	0.4098	0.0013	0.10505	0.00040	0.10497	0.00040
6266-22.2	5.989	0.043	2.455	0.020	1.00e−05	1.00e−05	0.3117	0.0014	7.253	0.029	2.974	0.016	0.04297	0.00015	0.19299	0.00068	0.4100	0.0018	0.10481	0.00052	0.10479	0.00052
6266-22.3	6.023	0.040	2.477	0.017	4.56e−05	6.55e−05	0.3055	0.0012	7.231	0.025	2.973	0.011	0.04226	0.00015	0.19511	0.00075	0.4112	0.0014	0.10277	0.00041	0.10269	0.00043
6266-23.1	6.327	0.029	2.582	0.013	8.00e−06	2.49e−05	0.3008	0.0012	7.257	0.031	2.962	0.014	0.04145	0.00019	0.19638	0.00087	0.4081	0.0021	0.10156	0.00051	0.10149	0.00060
6266-23.2	6.206	0.028	2.514	0.014	1.01e−05	2.02e−05	0.3124	0.0012	7.245	0.027	2.935	0.015	0.04312	0.00017	0.19703	0.00080	0.4051	0.0021	0.10643	0.00055	0.10638	0.00056
6266-23.3	6.254	0.024	2.571	0.011	1.76e−05	3.80e−05	0.3144	0.0016	7.286	0.030	2.995	0.014	0.04315	0.00018	0.19627	0.00084	0.4111	0.0014	0.10497	0.00049	0.10489	0.00049
6266-24.1	6.109	0.045	2.452	0.019	1.00e−05	1.00e−05	0.2860	0.0015	7.147	0.021	2.869	0.010	0.04002	0.00019	0.19532	0.00071	0.4013	0.0013	0.09970	0.00052	0.09967	0.00052
6266-24.2	6.257	0.026	2.539	0.021	7.53e−06	2.43e−05	0.3094	0.0019	7.389	0.036	2.998	0.026	0.04187	0.00021	0.19564	0.00079	0.4057	0.0032	0.10320	0.00090	0.10314	0.00090
6266-25.1	5.917	0.035	2.426	0.013	5.48e−05	2.12e−05	0.3153	0.0024	7.296	0.032	2.991	0.014	0.04322	0.00034	0.19321	0.00089	0.4100	0.0018	0.10541	0.00080	0.10531	0.00080
6266-25.2	5.950	0.032	2.407	0.010	5.78e−05	3.25e−05	0.3039	0.0013	7.142	0.036	2.889	0.010	0.04255	0.00024	0.19480	0.00102	0.4046	0.0021	0.10517	0.00047	0.10506	0.00048
6266-25.3	5.902	0.023	2.386	0.011	1.00e−05	1.00e−05	0.3010	0.0016	7.180	0.036	2.903	0.016	0.04192	0.00015	0.19462	0.00075	0.4043	0.0015	0.10370	0.00046	0.10368	0.00046
6266-26.1	6.122	0.027	2.483	0.016	1.00e−05	1.00e−05	0.2984	0.0012	7.234	0.024	2.933	0.017	0.04125	0.00014	0.19473	0.00107	0.4055	0.0022	0.10172	0.00060	0.10168	0.00060
6266-26.2	5.998	0.022	2.444	0.010	3.27e−05	2.76e−05	0.3095	0.0023	7.154	0.022	2.915	0.011	0.04326	0.00032	0.19445	0.00103	0.4074	0.0013	0.10618	0.00081	0.10612	0.00081
6266-26.3	6.039	0.024	2.466	0.011	2.64e−05	2.09e−05	0.3112	0.0025	7.329	0.040	2.993	0.017	0.04246	0.00028	0.19418	0.00073	0.4084	0.0014	0.10396	0.00071	0.10391	0.00071
6266-27.1	6.242	0.023	2.534	0.010	1.64e−05	1.53e−05	0.3084	0.0018	7.273	0.025	2.953	0.011	0.04240	0.00024	0.19625	0.00111	0.4060	0.0013	0.10445	0.00061	0.10438	0.00061
6266-27.2	6.208	0.038	2.537	0.016	3.02e−05	1.55e−05	0.3128	0.0012	7.251	0.024	2.963	0.011	0.04313	0.00016	0.19651	0.00071	0.4086	0.0015	0.10556	0.00042	0.10547	0.00042
6266-27.3	6.156	0.027	2.534	0.013	1.04e−05	1.61e−05	0.3135	0.0013	7.341	0.027	3.022	0.013	0.04270	0.00021	0.19516	0.00084	0.4117	0.0018	0.10371	0.00047	0.10367	0.00047
6266-28.1	5.884	0.030	2.448	0.011	3.31e−05	1.65e−05	0.3194	0.0016	7.328	0.036	3.049	0.012	0.04358	0.00025	0.19172	0.00096	0.4161	0.0021	0.10474	0.00054	0.10468	0.00054
6266-28.2	5.943	0.022	2.410	0.010	3.92e−05	2.55e−05	0.3070	0.0020	7.240	0.024	2.936	0.012	0.04241	0.00026	0.19145	0.00069	0.4056	0.0014	0.10456	0.00068	0.10449	0.00068
6266-28.3	5.888	0.044	2.395	0.014	3.47e−05	2.85e−05	0.3182	0.0013	7.296	0.026	2.968	0.012	0.04361	0.00017	0.19056	0.00116	0.4068	0.0016	0.10722	0.00044	0.10716	0.00045
6266-29.1	5.980	0.022	2.451	0.010	2.16e−05	1.65e−05	0.3071	0.0012	7.246	0.022	2.969	0.011	0.04239	0.00014	0.19461	0.00089	0.4098	0.0013	0.10343	0.00040	0.10343	0.00040
6266-29.2	5.949	0.023	2.418	0.010	2.77e−05	3.52e−05	0.3097	0.0013	7.241	0.027	2.943	0.012	0.04277	0.00015	0.19360	0.00073	0.4065	0.0013	0.10522	0.00041	0.10517	0.00042
6266-29.3	5.965	0.035	2.426	0.015	2.94e−05	1.62e−05	0.3004	0.0020	7.218	0.040	2.936	0.017	0.04161	0.00022	0.19673	0.00091	0.4067	0.0017	0.10231	0.00058	0.10226	0.00058
6266-30.1	6.017	0.032	2.450	0.011	1.93e−05	1.90e−05	0.3036	0.0013	7.160	0.027	2.916	0.012	0.04240	0.00017	0.19622	0.00074	0.4073	0.0014	0.10412	0.00042	0.10409	0.00042
6266-30.2	6.096	0.034	2.481	0.015	1.14e−05	1.40e−05	0.3151	0.0013	7.267	0.023	2.958	0.011	0.04336	0.00016	0.19569	0.00070	0.4071	0.0014	0.10651	0.00043	0.10648	0.00043
6266-31.1	6.075	0.026	2.496	0.011	1.47e−05	1.23e−05	0.3115	0.0015	7.277	0.032	2.990	0.013	0.04280	0.00018	0.19471	0.00091	0.4108	0.0015	0.10418	0.00045	0.10414	0.00045
6266-31.2	6.157	0.023	2.494	0.010	7.58e−06	1.60e−05	0.3111	0.0018	7.285	0.032	2.951	0.014	0.04271	0.00020	0.19358	0.00095	0.4051	0.0013	0.10543	0.00052	0.10539	0.00052
6266-31.3	6.144	0.029	2.531	0.013	2.47e−05	2.35e−05	0.3140	0.0021	7.324	0.027	3.017	0.013	0.04288	0.00026	0.19489	0.00075	0.4120	0.0014	0.10406	0.00068	0.10399	0.00068
6266-32.1	6.181	0.034	2.519	0.015	4.31e−05	2.68e−05	0.3102	0.0014	7.246	0.030	2.953	0.014	0.04281	0.00016	0.19451	0.00097	0.4076	0.0016	0.10502	0.00048	0.10491	0.00048
6266-32.2	6.154	0.043	2.528	0.019	5.45e−06	1.72e−05	0.3197	0.0014	7.286	0.025	2.993	0.013	0.04387	0.00017	0.19676	0.00126	0.4108	0.0016	0.10680	0.00050	0.10676	0.00050
6266-32.3	6.078	0.031	2.441	0.014	3.93e−05	3.35e−05	0.3077	0.0016	7.187	0.023	2.886	0.011	0.04281	0.00021	0.19646	0.00070	0.4016	0.0014	0.10662	0.00057	0.10654	0.00057
6266-33.1	6.239	0.026	2.559	0.012	2.81e−05	1.96e−05	0.3123	0.0013	7.354	0.025	3.016	0.013	0.04247	0.00016	0.19640	0.00080	0.4102	0.0016	0.10353	0.00047	0.10344	0.00047
6266-33.2	6.181	0.029	2.530	0.015	1.28e−05	1.86e−05	0.3106	0.0024	7.261	0.028	2.973	0.015	0.04278	0.00031	0.19333	0.00071	0.4094	0.0018	0.10448	0.00083	0.10445	0.00083
6266-34.1	6.032	0.023	2.445	0.010	2.84e−06	2.39e−05	0.3051	0.0013	7.167	0.024	2.906	0.011	0.04256	0.00014	0.19485	0.00070	0.4054	0.0013	0.10499	0.00043	0.10498	0.00043
6266-34.2	6.086	0.048	2.481	0.020	5.42e−05	2.56e−05	0.3124	0.0017	7.203	0.025	2.936	0.012	0.04337	0.00022	0.19394	0.00132	0.4076	0.0014	0.10642	0.00058	0.10631	0.00058
6266-35.1	6.108	0.039	2.505	0.016	2.31e−05	2.60e−05	0.3142	0.0015	7.233	0.039	2.966	0.017	0.04344	0.00020	0.19698	0.00153	0.4101	0.0022	0.10593	0.00052	0.10587	0.00052
6266-35.2	6.069	0.025	2.481	0.014	1.37e−05	1.90e−05	0.3132	0.0015	7.178	0.023	2.934	0.015	0.04363	0.00019	0.19524	0.00126	0.4088	0.0020	0.10673	0.00063	0.10670	0.00063
6266-36.1	6.241	0.027	2.551	0.012	2.43e−05	1.37e−05	0.3071	0.0013	7.239	0.027	2.959	0.012	0.04242	0.00020	0.19559	0.00084	0.4087	0.0018	0.10378	0.00051	0.10369	0.00051
6266-36.2	6.256	0.036	2.548	0.014	3.42e−05	2.27e−05	0.3040	0.0019	7.143	0.032	2.909	0.012	0.04256	0.00027	0.19718	0.00084	0.4073	0.0017	0.10451	0.00065	0.10440	0.00065
6266-36.3	6.311	0.032	2.582	0.013	1.00e−05	1.00e−05	0.3107	0.0021	7.270	0.030	2.974	0.012	0.04274	0.00029	0.19641	0.00104	0.4091	0.0016	0.10449	0.00069	0.10442	0.00069
6266-37.1	6.325	0.028	2.609	0.012	3.27e−05	2.77e−05	0.3009	0.0017	7.335	0.040	3.026	0.019	0.04102	0.00018	0.19714	0.00101	0.4125	0.0021	0.09945	0.00054	0.09939	0.00054
6266-37.2	6.338	0.025	2.559	0.011	2.02e−05	1.52e−05	0.3019	0.0013	7.272	0.025	2.936	0.012	0.04152	0.00015	0.19334	0.00074	0.4038	0.0014	0.10282	0.00043	0.10272	0.00043
6266-37.3	6.342	0.046	2.583	0.021	1.65e−05	2.06e−05	0.3076	0.0021	7.253	0.024	2.953	0.014	0.04241	0.00027	0.19580	0.00069	0.4072	0.0018	0.10413	0.00076	0.10404	0.00076
6266-38.1	6.148	0.027	2.472	0.014	1.00e−05	1.00e−05	0.2930	0.0011	7.193	0.022	2.892	0.014	0.04074	0.00015	0.19509	0.00066	0.4020	0.0018	0.10134	0.00051	0.10130	0.00052
6266-38.2	6.143	0.025	2.507	0.016	6.05e−05	2.83e−05	0.3112	0.0019	7.255	0.042	2.961	0.022	0.04290	0.00014	0.19471	0.00159	0.4082	0.0022	0.10510	0.00060	0.10497	0.00060
6266-39.1	6.226	0.034	2.552	0.015	1.98e−05	2.04e−05	0.3099	0.0022	7.220	0.046	2.960	0.020	0.04292	0.00018	0.19581	0.00067	0.4099	0.0014	0.10471	0.00050	0.10463	0.00051
6266-39.2	6.226	0.029	2.555	0.012	8.55e−06	1.01e−05	0.3147	0.0012	7.327	0.025	3.008	0.011	0.04294	0.00016	0.19498	0.00109	0.4104	0.0014	0.10462	0.00041	0.10457	0.00041
6266-39.3	6.230	0.024	2.538	0.011	1.99e−05	2.26e−05	0.3070	0.0018	7.217	0.039	2.940	0.017	0.04253	0.00016	0.19554	0.00072	0.4074	0.0013	0.10441	0.00043	0.10433	0.00043
6266-40.1	6.101	0.036	2.491	0.018	1.00e−05	1.00e−05	0.3066	0.0015	7.376	0.032	3.012	0.018	0.04157	0.00014	0.19358	0.00085	0.4083	0.0020	0.10180	0.00054	0.10177	0.00054
6266-40.2	6.097	0.050	2.483	0.021	8.33e−06	2.59e−05	0.3124	0.0022	7.283	0.027	2.966	0.013	0.04290	0.00028	0.19331	0.00069	0.4072	0.0013	0.10535	0.00071	0.10532	0.00071
6266-40.3	6.070	0.027	2.473	0.012	5.89e−06	7.99e−06	0.3076	0.0014	7.271	0.029	2.963	0.013	0.04231	0.00021	0.19569	0.00084	0.4075	0.0019	0.10383	0.00054	0.10381	0.00054
6266-41.1	6.007	0.028	2.447	0.010	7.23e−06	1.57e−05	0.3133	0.0013	7.261	0.033	2.958	0.012	0.04314	0.00019	0.19301	0.00086	0.4074	0.0017	0.10590	0.00042	0.10589	0.00042
6266-41.2	6.067	0.051	2.486	0.021	7.98e−06	1.46e−05	0.3104	0.0022	7.263	0.032	2.976	0.014	0.04273	0.00026	0.19386	0.00068	0.4098	0.0013	0.10428	0.00068	0.10426	0.00068

Table 4 (*continued*)

Analysis (6266-grain#.spot#)	$^{254}U/^{196}Zr$	$\pm^{254}U/^{196}Zr$	$^{270}U/^{196}Zr$	$\pm^{270}U/^{196}Zr$	$^{204}Pb/^{206}Pb$	$\pm^{204}Pb/^{206}Pb$	$^{206}Pb/^{238}U$	$\pm^{206}Pb/^{238}U$	$^{254}U/^{238}U$	$\pm^{254}U/^{238}U$	$^{270}U/^{238}U$	$\pm^{270}U/^{238}U$	$^{206}Pb/^{254}U$	$\pm^{206}Pb/^{254}U$	$^{248}Th/^{254}U$	$\pm^{248}Th/^{254}U$	$^{270}U/^{254}U$	$\pm^{270}U/^{254}U$	$^{206}Pb/^{270}U$	$\pm^{206}Pb/^{270}U$	$^{206}Pb*/^{270}U$	$\pm^{206}Pb*/^{270}U$
6266-41.3	5.969	0.023	2.438	0.010	5.72e−06	7.98e−06	0.3165	0.0022	7.272	0.024	2.970	0.011	0.04352	0.00030	0.19359	0.00072	0.4083	0.0014	0.10658	0.00075	0.10657	0.00075
6266-42.1	5.969	0.022	2.414	0.018	1.33e−05	2.51e−05	0.2983	0.0016	7.203	0.022	2.912	0.021	0.04142	0.00021	0.19557	0.00071	0.4043	0.0029	0.10244	0.00085	0.10242	0.00085
6266-42.2	5.982	0.023	2.446	0.011	3.32e−05	2.14e−05	0.3099	0.0013	7.243	0.023	2.962	0.011	0.04278	0.00017	0.19413	0.00070	0.4089	0.0015	0.10463	0.00048	0.10457	0.00048
6266-43.1	5.996	0.025	2.441	0.011	7.92e−06	2.40e−05	0.3059	0.0021	7.235	0.023	2.945	0.011	0.04228	0.00028	0.19595	0.00070	0.4071	0.0014	0.10385	0.00072	0.10384	0.00072
6266-43.2	5.986	0.044	2.461	0.019	5.02e−06	2.37e−05	0.3137	0.0017	7.290	0.028	2.997	0.013	0.04303	0.00021	0.19291	0.00069	0.4111	0.0013	0.10467	0.00054	0.10466	0.00054
6266-44.1	5.949	0.022	2.419	0.010	1.00e−05	1.00e−05	0.3040	0.0013	7.186	0.022	2.921	0.011	0.04231	0.00017	0.19432	0.00086	0.4065	0.0014	0.10407	0.00047	0.10405	0.00047
6266-44.2	5.970	0.022	2.437	0.015	1.88e−05	1.63e−05	0.3087	0.0020	7.208	0.033	2.942	0.020	0.04283	0.00022	0.19255	0.00123	0.4082	0.0023	0.10491	0.00076	0.10488	0.00076
6266-44.3	5.907	0.023	2.402	0.011	4.22e−05	2.34e−05	0.3090	0.0014	7.205	0.027	2.930	0.013	0.04290	0.00016	0.19341	0.00134	0.4066	0.0015	0.10549	0.00046	0.10541	0.00047
6266-45.1	5.978	0.024	2.428	0.011	2.57e−05	2.89e−05	0.2933	0.0022	7.242	0.022	2.941	0.011	0.04049	0.00030	0.19630	0.00106	0.4062	0.0013	0.09970	0.00077	0.09965	0.00077
6266-45.2	5.940	0.022	2.427	0.010	1.19e−05	2.00e−05	0.3066	0.0012	7.228	0.023	2.953	0.011	0.04243	0.00015	0.19453	0.00073	0.4086	0.0013	0.10382	0.00041	0.10380	0.00041
6266-45.3	6.007	0.024	2.471	0.011	4.33e−05	4.17e−05	0.3060	0.0014	7.286	0.031	2.998	0.014	0.04200	0.00016	0.19534	0.00147	0.4114	0.0015	0.10208	0.00042	0.10200	0.00042
6266-46.1	5.981	0.022	2.454	0.017	3.39e−05	2.69e−05	0.3053	0.0019	7.294	0.041	2.993	0.025	0.04186	0.00014	0.19405	0.00076	0.4103	0.0027	0.10201	0.00071	0.10195	0.00071
6266-46.2	5.974	0.035	2.425	0.012	1.86e−05	1.23e−05	0.3130	0.0018	7.245	0.041	2.941	0.014	0.04320	0.00026	0.19373	0.00100	0.4059	0.0020	0.10644	0.00054	0.10641	0.00054
6266-46.3	5.962	0.025	2.436	0.011	3.43e−05	2.34e−05	0.3145	0.0013	7.234	0.027	2.955	0.012	0.04347	0.00018	0.19377	0.00079	0.4085	0.0016	0.10642	0.00046	0.10636	0.00046
6266-47.1	6.216	0.025	2.536	0.013	2.08e−05	2.11e−05	0.3108	0.0019	7.309	0.041	2.982	0.019	0.04252	0.00014	0.19439	0.00074	0.4079	0.0017	0.10423	0.00049	0.10416	0.00049
6266-47.2	6.192	0.030	2.528	0.011	2.32e−05	2.22e−05	0.3145	0.0025	7.225	0.031	2.949	0.011	0.04353	0.00037	0.19501	0.00089	0.4082	0.0019	0.10664	0.00087	0.10656	0.00087
6266-48.1	5.964	0.031	2.457	0.014	4.16e−05	2.16e−05	0.3128	0.0012	7.288	0.022	3.003	0.011	0.04291	0.00014	0.19554	0.00068	0.4120	0.0013	0.10415	0.00040	0.10407	0.00040
6266-48.2	6.050	0.024	2.478	0.011	3.09e−06	1.92e−05	0.3160	0.0013	7.335	0.024	3.004	0.011	0.04308	0.00016	0.19453	0.00076	0.4096	0.0014	0.10519	0.00043	0.10518	0.00043
6266-49.1	6.102	0.029	2.521	0.011	1.15e−05	2.10e−05	0.3209	0.0017	7.333	0.040	3.030	0.016	0.04376	0.00019	0.19527	0.00088	0.4132	0.0018	0.10590	0.00044	0.10586	0.00044
6266-49.2	6.007	0.040	2.448	0.017	1.47e−05	1.22e−05	0.3188	0.0014	7.254	0.027	2.955	0.012	0.04395	0.00016	0.19457	0.00070	0.4074	0.0014	0.10787	0.00044	0.10784	0.00044
6266-49.3	6.080	0.031	2.495	0.016	2.04e−05	1.63e−05	0.3093	0.0014	7.232	0.037	2.968	0.020	0.04277	0.00021	0.19590	0.00096	0.4104	0.0028	0.10420	0.00066	0.10415	0.00066
6266-50.1	5.987	0.028	2.446	0.014	5.61e−05	2.46e−05	0.3078	0.0012	7.282	0.022	2.974	0.013	0.04227	0.00014	0.19640	0.00079	0.4085	0.0017	0.10349	0.00048	0.10339	0.00048
6266-50.2	5.961	0.037	2.423	0.016	4.60e−06	2.36e−05	0.3054	0.0024	7.190	0.024	2.923	0.011	0.04248	0.00033	0.19340	0.00122	0.4065	0.0013	0.10451	0.00083	0.10450	0.00083
6266-50.3	6.017	0.023	2.459	0.012	1.48e−05	2.15e−05	0.3107	0.0013	7.233	0.025	2.955	0.012	0.04296	0.00020	0.19461	0.00146	0.4086	0.0015	0.10513	0.00045	0.10510	0.00045
6266-51.1	6.061	0.026	2.471	0.012	1.00e−05	1.00e−05	0.3056	0.0019	7.226	0.022	2.946	0.011	0.04229	0.00025	0.19663	0.00068	0.4077	0.0013	0.10375	0.00064	0.10373	0.00064
6266-51.2	6.104	0.026	2.501	0.014	3.05e−05	2.10e−05	0.3029	0.0015	7.275	0.028	2.981	0.015	0.04163	0.00022	0.19526	0.00136	0.4097	0.0022	0.10161	0.00063	0.10154	0.00063
6266-51.3	6.164	0.024	2.507	0.011	1.27e−05	2.43e−05	0.2991	0.0026	7.275	0.054	2.958	0.023	0.04111	0.00022	0.19702	0.00077	0.4067	0.0014	0.10110	0.00058	0.10105	0.00058
6266-52.1	6.012	0.032	2.452	0.012	1.00e−05	1.00e−05	0.3053	0.0017	7.242	0.028	2.953	0.011	0.04216	0.00025	0.19401	0.00114	0.4078	0.0016	0.10337	0.00060	0.10335	0.00060
6266-52.2	6.045	0.029	2.466	0.011	1.49e−05	2.24e−05	0.3141	0.0020	7.240	0.032	2.954	0.011	0.04339	0.00030	0.19492	0.00094	0.4080	0.0018	0.10634	0.00069	0.10631	0.00069
6266-53.1	5.970	0.034	2.441	0.013	1.14e−05	1.78e−05	0.3115	0.0015	7.298	0.037	2.984	0.013	0.04268	0.00025	0.19239	0.00103	0.4089	0.0024	0.10438	0.00057	0.10436	0.00057
6266-53.2	5.963	0.022	2.416	0.010	4.85e−05	2.91e−05	0.3094	0.0018	7.288	0.030	2.953	0.013	0.04245	0.00021	0.19204	0.00100	0.4052	0.0013	0.10478	0.00056	0.10469	0.00056
6266-53.3	5.963	0.025	2.434	0.011	3.12e−05	2.88e−05	0.3007	0.0015	7.232	0.024	2.952	0.011	0.04158	0.00020	0.19494	0.00071	0.4082	0.0014	0.10186	0.00052	0.10180	0.00052
6266-55.1	6.243	0.028	2.526	0.011	1.70e−05	1.76e−05	0.3050	0.0012	7.267	0.028	2.940	0.011	0.04197	0.00018	0.19793	0.00081	0.4046	0.0016	0.10374	0.00043	0.10367	0.00043

6266-55.2	6.182	0.027	2.506	0.014	2.33e−05	2.28e−05	0.3095	0.0011	7.278	0.024	2.950	0.013	0.04252	0.00015	0.19565	0.00126	0.4053	0.0018	0.10491	0.00050	0.10484	0.00050
6266-55.3	6.113	0.026	2.491	0.012	1.00e−05	1.00e−05	0.3010	0.0015	7.237	0.023	2.948	0.012	0.04159	0.00020	0.19716	0.00070	0.4074	0.0015	0.10209	0.00054	0.10206	0.00054
6266-56.1	6.309	0.056	2.595	0.027	7.59e−06	1.60e−05	0.3089	0.0013	7.315	0.028	3.009	0.019	0.04223	0.00014	0.19635	0.00067	0.4113	0.0024	0.10267	0.00063	0.10260	0.00063
6266-56.2	6.196	0.026	2.540	0.012	1.86e−05	1.48e−05	0.3170	0.0016	7.314	0.023	2.998	0.011	0.04334	0.00021	0.19498	0.00069	0.4100	0.0013	0.10571	0.00054	0.10564	0.00054
6266-56.3	6.239	0.026	2.577	0.017	3.36e−05	3.41e−05	0.3165	0.0013	7.240	0.023	2.990	0.018	0.04371	0.00016	0.19555	0.00094	0.4131	0.0024	0.10583	0.00067	0.10573	0.00067
6266-57.1	6.166	0.051	2.533	0.019	1.63e−06	3.02e−05	0.3137	0.0014	7.246	0.038	2.977	0.012	0.04299	0.00025	0.19516	0.00124	0.4108	0.0023	0.10538	0.00051	0.10535	0.00051
6266-57.2	6.224	0.025	2.543	0.014	1.69e−05	1.55e−05	0.3121	0.0012	7.261	0.026	2.967	0.018	0.04299	0.00016	0.19505	0.00075	0.4086	0.0024	0.10520	0.00064	0.10513	0.00064
6266-57.3	6.163	0.041	2.520	0.018	1.53e−05	2.95e−05	0.3131	0.0012	7.251	0.023	2.964	0.011	0.04318	0.00015	0.19472	0.00091	0.4088	0.0014	0.10563	0.00042	0.10557	0.00042
6266-58.1	6.068	0.046	2.488	0.019	1.00e−05	1.00e−05	0.3023	0.0018	7.274	0.032	2.982	0.014	0.04156	0.00028	0.19375	0.00092	0.4100	0.0022	0.10137	0.00070	0.10134	0.00070
6266-58.2	5.991	0.029	2.446	0.013	1.00e−05	1.00e−05	0.3154	0.0012	7.210	0.023	2.944	0.011	0.04374	0.00015	0.19393	0.00075	0.4083	0.0014	0.10715	0.00042	0.10713	0.00042
6266-58.3	6.070	0.043	2.471	0.018	1.00e−05	1.00e−05	0.3103	0.0013	7.194	0.023	2.928	0.011	0.04313	0.00016	0.19372	0.00077	0.4070	0.0014	0.10598	0.00044	0.10595	0.00044
6266-59.1	6.128	0.028	2.484	0.012	3.82e−06	2.15e−05	0.2980	0.0026	7.176	0.030	2.909	0.013	0.04152	0.00035	0.19483	0.00093	0.4054	0.0014	0.10244	0.00087	0.10241	0.00087
6266-59.2	6.191	0.041	2.491	0.012	1.72e−05	4.78e−05	0.3027	0.0011	7.255	0.046	2.919	0.013	0.04172	0.00027	0.19484	0.00163	0.4023	0.0028	0.10371	0.00048	0.10365	0.00049
6266-60.1	6.002	0.039	2.452	0.013	2.31e−05	1.35e−05	0.3052	0.0019	7.193	0.038	2.939	0.012	0.04243	0.00029	0.19496	0.00119	0.4086	0.0020	0.10384	0.00062	0.10380	0.00062
6266-60.2	5.994	0.024	2.456	0.012	4.93e−05	2.70e−05	0.3099	0.0013	7.221	0.028	2.959	0.013	0.04291	0.00016	0.19310	0.00081	0.4097	0.0017	0.10474	0.00046	0.10465	0.00046
6266-60.3	5.981	0.032	2.428	0.016	1.38e−05	3.00e−05	0.3054	0.0012	7.258	0.032	2.947	0.017	0.04208	0.00020	0.19379	0.00092	0.4061	0.0026	0.10362	0.00062	0.10360	0.00062
6266-61.1	6.114	0.028	2.472	0.010	4.79e−05	2.22e−05	0.3022	0.0011	7.256	0.029	2.934	0.011	0.04165	0.00018	0.19658	0.00085	0.4043	0.0017	0.10301	0.00041	0.10291	0.00041
6266-61.2	6.156	0.023	2.487	0.011	4.70e−05	1.93e−05	0.3131	0.0013	7.215	0.026	2.915	0.013	0.04340	0.00015	0.19389	0.00127	0.4040	0.0015	0.10740	0.00047	0.10729	0.00047
6266-61.3	6.111	0.035	2.476	0.015	1.00e−05	1.00e−05	0.3125	0.0020	7.352	0.039	2.979	0.017	0.04251	0.00019	0.19441	0.00069	0.4052	0.0013	0.10491	0.00051	0.10488	0.00051
6266-62.1	5.954	0.025	2.454	0.011	3.81e−05	1.78e−05	0.3129	0.0018	7.275	0.027	2.998	0.012	0.04302	0.00025	0.19516	0.00077	0.4122	0.0016	0.10437	0.00062	0.10430	0.00062
6266-62.2	5.975	0.028	2.435	0.011	1.00e−05	1.00e−05	0.2951	0.0012	7.214	0.029	2.940	0.011	0.04090	0.00018	0.19503	0.00087	0.4075	0.0017	0.10038	0.00040	0.10036	0.00040
6266-62.3	5.994	0.024	2.398	0.013	1.71e−05	1.36e−05	0.2935	0.0017	7.131	0.039	2.853	0.019	0.04116	0.00014	0.19413	0.00091	0.4001	0.0018	0.10286	0.00052	0.10283	0.00052
Average	6.068		2.470		0.000022		0.3067		7.225		2.941		0.04245		0.1949		0.4070		0.1043		0.1042	
Standard deviation	0.122		0.056		0.000016		0.0077		0.086		0.055		0.00080		0.0014		0.0033		0.0017		0.0017	
Standard deviation (%)	2.01		2.28		73.21		2.51		1.20		1.86		1.89		0.69		0.80		1.64		1.64	
Standard error	0.0096		0.0044		0.0000012		0.00061		0.0068		0.0043		0.00006		0.00011		0.00026		0.00014		0.00013	
Standard error (%)	0.16		0.18		5.77		0.20		0.09		0.15		0.15		0.05		0.06		0.13		0.13	
Skew	0.09		− 0.14		0.99		− 1.01		− 1.30		− 1.28		− 0.64		− 0.32		− 0.76		− 0.35		− 0.35	
Kurtosis	− 0.71		− 0.01		0.34		1.47		1.89		1.93		0.35		0.25		1.32		0.10		0.10	
Avg. error (%)	0.49		0.54		97.48		0.51		0.41		0.47		0.47		0.47		0.42		0.53		0.53	

Table 5
Raw SHRIMP isotopic data (± 1σ) for z6266 zircon, experiment IP222.2

Analysis (6266-grain#.spot#)	$^{254}U/^{196}Zr$	$\pm^{254}U/^{196}Zr$	$^{270}U/^{196}Zr$	$\pm^{270}U/^{196}Zr$	$^{204}Pb/^{206}Pb$	$\pm^{204}Pb/^{206}Pb$	$^{206}Pb/^{238}U$	$\pm^{206}Pb/^{238}U$	$^{254}U/^{238}U$	$\pm^{254}U/^{238}U$	$^{270}U/^{238}U$	$\pm^{270}U/^{238}U$	$^{206}Pb/^{254}U$	$\pm^{206}Pb/^{254}U$	$^{248}Th/^{254}U$	$\pm^{248}Th/^{254}U$	$^{270}U/^{254}U$	$\pm^{270}U/^{254}U$	$^{206}Pb/^{270}U$	$\pm^{206}Pb/^{270}U$	$^{206}Pb*/^{270}U$	$\pm^{206}Pb*/^{270}U$
6266-20.4	6.069	0.025	2.486	0.013	2.21e−05	2.32e−05	0.3100	0.0015	7.292	0.029	2.987	0.016	0.04251	0.00019	0.19378	0.00124	0.4097	0.0020	0.10376	0.00057	0.10371	0.00057
6266-20.5	6.077	0.024	2.467	0.011	9.37e−05	3.11e−05	0.3014	0.0012	7.248	0.025	2.942	0.012	0.04158	0.00015	0.19360	0.00070	0.4059	0.0014	0.10243	0.00042	0.10225	0.00042
6266-20.6	6.159	0.037	2.484	0.013	4.12e−05	3.29e−05	0.2986	0.0015	7.226	0.038	2.914	0.012	0.04132	0.00024	0.19555	0.00104	0.4033	0.0021	0.10246	0.00050	0.10236	0.00050
6266-20.7	6.165	0.023	2.513	0.011	5.45e−06	1.54e−05	0.3144	0.0016	7.371	0.024	3.004	0.011	0.04265	0.00020	0.19325	0.00094	0.4076	0.0013	0.10464	0.00053	0.10460	0.00053
6266-27.4	6.178	0.025	2.532	0.011	1.66e−05	1.72e−05	0.3100	0.0021	7.337	0.029	3.007	0.013	0.04225	0.00026	0.19474	0.00068	0.4098	0.0013	0.10308	0.00065	0.10302	0.00065
6266-27.5	6.185	0.026	2.520	0.011	3.02e−05	7.36e−05	0.3093	0.0020	7.305	0.041	2.976	0.018	0.04235	0.00019	0.19481	0.00076	0.4074	0.0016	0.10394	0.00050	0.10385	0.00052
6266-27.6	6.180	0.048	2.505	0.023	1.07e−05	1.70e−05	0.3083	0.0026	7.267	0.040	2.946	0.022	0.04242	0.00030	0.19457	0.00072	0.4054	0.0024	0.10465	0.00091	0.10460	0.00091
6266-27.7	6.204	0.052	2.489	0.021	1.15e−05	1.60e−05	0.2938	0.0014	7.170	0.023	2.876	0.011	0.04098	0.00018	0.19529	0.00092	0.4012	0.0013	0.10216	0.00050	0.10211	0.00050
6266-28.4	5.872	0.024	2.357	0.012	6.06e−05	2.33e−05	0.2972	0.0014	7.160	0.025	2.874	0.013	0.04150	0.00018	0.19170	0.00071	0.4014	0.0016	0.10340	0.00054	0.10329	0.00054
6266-28.5	5.895	0.023	2.380	0.011	4.02e−05	2.78e−05	0.3009	0.0013	7.224	0.024	2.917	0.011	0.04165	0.00017	0.19231	0.00142	0.4038	0.0014	0.10314	0.00046	0.10307	0.00047
6266-28.6	5.943	0.035	2.448	0.020	1.00e−05	1.00e−05	0.3134	0.0030	7.303	0.050	3.007	0.027	0.04292	0.00036	0.19183	0.00089	0.4118	0.0031	0.10421	0.00105	0.10419	0.00105
6266-28.7	5.888	0.028	2.384	0.010	1.00e−05	1.00e−05	0.2918	0.0017	7.180	0.033	2.907	0.012	0.04063	0.00025	0.19343	0.00090	0.4048	0.0018	0.10038	0.00057	0.10036	0.00057
6266-28.7.2 (replicate)	5.866	0.031	2.382	0.012	1.40e−05	2.09e−05	0.3001	0.0021	7.237	0.051	2.939	0.020	0.04146	0.00018	0.19277	0.00085	0.4061	0.0017	0.10211	0.00042	0.10209	0.00042
6266-29.4	6.012	0.024	2.430	0.012	5.76e−06	1.62e−05	0.2984	0.0016	7.219	0.029	2.918	0.015	0.04133	0.00018	0.19385	0.00145	0.4042	0.0016	0.10225	0.00054	0.10224	0.00054
6266-29.5	6.025	0.025	2.441	0.011	1.06e−05	2.89e−05	0.3061	0.0015	7.196	0.032	2.915	0.014	0.04253	0.00018	0.19318	0.00083	0.4051	0.0016	0.10499	0.00047	0.10497	0.00048
6266-31.4	6.134	0.040	2.500	0.018	3.38e−05	3.71e−05	0.3046	0.0017	7.249	0.037	2.954	0.017	0.04201	0.00016	0.19427	0.00083	0.4075	0.0017	0.10311	0.00050	0.10303	0.00050
6266-31.5	6.110	0.031	2.473	0.018	2.80e−05	2.16e−05	0.2989	0.0021	7.188	0.025	2.909	0.018	0.04158	0.00028	0.19422	0.00079	0.4047	0.0023	0.10274	0.00086	0.10267	0.00086
6266-31.6	6.125	0.029	2.499	0.014	1.50e−05	2.45e−05	0.3106	0.0019	7.313	0.044	2.984	0.020	0.04247	0.00015	0.19333	0.00073	0.4081	0.0017	0.10408	0.00047	0.10403	0.00047
6266-32.4	6.129	0.028	2.492	0.011	3.14e−05	2.07e−05	0.3027	0.0018	7.182	0.028	2.921	0.011	0.04215	0.00026	0.19594	0.00084	0.4067	0.0016	0.10365	0.00063	0.10357	0.00063
6266-32.5	6.162	0.044	2.494	0.024	2.03e−05	1.36e−05	0.3067	0.0024	7.205	0.047	2.917	0.026	0.04257	0.00022	0.19844	0.00076	0.4048	0.0028	0.10515	0.00084	0.10509	0.00084
6266-32.6	6.183	0.032	2.517	0.016	1.00e−05	1.00e−05	0.3131	0.0013	7.220	0.026	2.940	0.015	0.04336	0.00016	0.19525	0.00073	0.4072	0.0019	0.10649	0.00055	0.10644	0.00056
6266-32.6.2 (replicate)	6.179	0.029	2.471	0.011	4.67e−05	1.97e−05	0.3037	0.0022	7.168	0.045	2.867	0.018	0.04236	0.00024	0.19510	0.00113	0.3999	0.0016	0.10594	0.00059	0.10582	0.00059
6266-32.7	6.162	0.041	2.502	0.016	2.70e−05	2.97e−05	0.3062	0.0012	7.263	0.031	2.949	0.011	0.04216	0.00019	0.19535	0.00134	0.4060	0.0018	0.10384	0.00042	0.10376	0.00042
6266-36.4	6.258	0.026	2.564	0.012	1.00e−05	1.00e−05	0.3086	0.0016	7.223	0.036	2.960	0.016	0.04273	0.00014	0.19642	0.00075	0.4097	0.0016	0.10428	0.00043	0.10422	0.00043
6266-36.5	6.173	0.022	2.501	0.012	1.66e−05	2.20e−05	0.2985	0.0021	7.193	0.021	2.914	0.013	0.04149	0.00028	0.19587	0.00079	0.4051	0.0017	0.10243	0.00077	0.10237	0.00077
6266-36.5.2 (replicate)	6.167	0.051	2.520	0.021	6.60e−05	3.58e−05	0.3113	0.0013	7.233	0.025	2.956	0.012	0.04304	0.00015	0.19401	0.00077	0.4086	0.0015	0.10534	0.00044	0.10519	0.00044
6266-36.6	6.219	0.035	2.533	0.010	1.39e−05	3.54e−05	0.3039	0.0013	7.217	0.039	2.940	0.011	0.04211	0.00021	0.19583	0.00102	0.4073	0.0019	0.10338	0.00034	0.10332	0.00035
6266-37.4	6.246	0.041	2.561	0.017	2.68e−05	2.14e−05	0.3118	0.0015	7.324	0.032	3.003	0.013	0.04256	0.00020	0.19453	0.00095	0.4099	0.0018	0.10383	0.00050	0.10374	0.00050
6266-37.5	6.338	0.030	2.568	0.013	3.41e−05	2.58e−05	0.3049	0.0016	7.241	0.033	2.934	0.014	0.04210	0.00024	0.19518	0.00089	0.4052	0.0021	0.10392	0.00061	0.10380	0.00061
6266-37.6	6.337	0.043	2.572	0.018	1.00e−05	1.00e−05	0.2993	0.0013	7.177	0.027	2.912	0.012	0.04170	0.00015	0.19774	0.00084	0.4058	0.0015	0.10276	0.00043	0.10268	0.00043
6266-37.7	6.314	0.032	2.577	0.011	2.09e−05	3.26e−05	0.3074	0.0013	7.268	0.034	2.967	0.012	0.04229	0.00021	0.19577	0.00107	0.4082	0.0019	0.10360	0.00044	0.10351	0.00045
6266-38.3	6.104	0.051	2.495	0.021	1.94e−05	2.51e−05	0.3052	0.0013	7.247	0.027	2.962	0.011	0.04212	0.00017	0.19349	0.00076	0.4087	0.0014	0.10304	0.00044	0.10299	0.00044
6266-38.4	6.132	0.032	2.503	0.017	1.96e−05	2.34e−05	0.3025	0.0012	7.262	0.023	2.964	0.017	0.04165	0.00014	0.19526	0.00066	0.4082	0.0021	0.10203	0.00058	0.10198	0.00058

ID	C1		C2		C3		C4		C5		C6		C7		C8		C9		C10		C11	
6266-39.1	6.131	0.024	2.445	0.011	9.73e−06	9.59e−06	0.2848	0.0011	7.001	0.021	2.791	0.010	0.04068	0.00014	0.19662	0.00116	0.3987	0.0013	0.10201	0.00041	0.10197	0.00041
6266-39.2	6.220	0.030	2.543	0.013	6.20e−05	2.46e−05	0.3125	0.0014	7.308	0.035	2.988	0.015	0.04276	0.00020	0.19525	0.00126	0.4089	0.0021	0.10456	0.00051	0.10441	0.00051
6266-39.3	6.165	0.030	2.488	0.010	3.22e−06	2.69e−05	0.2954	0.0013	7.182	0.036	2.899	0.012	0.04113	0.00019	0.19458	0.00100	0.4036	0.0017	0.10189	0.00037	0.10186	0.00037
6266-40.3	6.014	0.040	2.418	0.017	4.98e−05	3.30e−05	0.2991	0.0012	7.186	0.030	2.889	0.013	0.04162	0.00019	0.19247	0.00092	0.4020	0.0020	0.10354	0.00049	0.10345	0.00049
6266-40.4	6.044	0.046	2.477	0.020	4.89e−06	2.34e−05	0.3133	0.0015	7.300	0.025	2.992	0.012	0.04292	0.00019	0.19222	0.00072	0.4099	0.0014	0.10473	0.00050	0.10472	0.00050
6266-40.5	6.073	0.024	2.456	0.016	1.11e−05	1.75e−05	0.3074	0.0023	7.245	0.047	2.930	0.024	0.04244	0.00020	0.19374	0.00080	0.4044	0.0024	0.10492	0.00073	0.10489	0.00073
6266-40.6	6.106	0.028	2.481	0.010	1.67e−05	2.29e−05	0.2998	0.0019	7.201	0.030	2.926	0.011	0.04163	0.00028	0.19553	0.00087	0.4064	0.0017	0.10245	0.00066	0.10241	0.00066
6266-41.4	6.000	0.036	2.420	0.013	5.55e−06	1.73e−05	0.2976	0.0012	7.160	0.038	2.887	0.013	0.04156	0.00023	0.19379	0.00111	0.4033	0.0023	0.10306	0.00048	0.10305	0.00048
6266-41.5	5.898	0.038	2.425	0.017	4.33e−05	2.12e−05	0.3106	0.0020	7.261	0.040	2.985	0.019	0.04278	0.00020	0.19345	0.00073	0.4111	0.0018	0.10407	0.00058	0.10399	0.00058
6266-44.4	5.996	0.025	2.428	0.013	1.91e−05	3.08e−05	0.2982	0.0016	7.204	0.034	2.917	0.017	0.04140	0.00015	0.19277	0.00103	0.4049	0.0017	0.10226	0.00050	0.10223	0.00050
6266-44.5	5.970	0.023	2.430	0.016	1.00e−05	1.00e−05	0.3024	0.0017	7.218	0.037	2.938	0.022	0.04189	0.00015	0.19325	0.00088	0.4070	0.0024	0.10292	0.00066	0.10290	0.00066
6266-44.6	5.922	0.028	2.413	0.012	1.11e−05	5.40e−05	0.3096	0.0016	7.217	0.026	2.941	0.012	0.04290	0.00021	0.19113	0.00088	0.4075	0.0016	0.10528	0.00057	0.10526	0.00058
6266-44.7	5.929	0.044	2.382	0.021	1.06e−05	2.55e−05	0.2945	0.0012	7.052	0.024	2.833	0.017	0.04176	0.00016	0.19370	0.00082	0.4017	0.0022	0.10397	0.00063	0.10395	0.00063
6266-45.4	6.011	0.026	2.406	0.011	2.85e−05	2.56e−05	0.2996	0.0012	7.265	0.029	2.908	0.012	0.04124	0.00017	0.19255	0.00150	0.4002	0.0016	0.10303	0.00042	0.10298	0.00043
6266-45.5	6.039	0.023	2.459	0.011	2.18e−05	3.37e−05	0.3050	0.0022	7.267	0.038	2.959	0.017	0.04197	0.00024	0.19364	0.00126	0.4073	0.0014	0.10305	0.00062	0.10301	0.00062
6266-45.6	5.991	0.034	2.452	0.015	1.00e−05	1.00e−05	0.3107	0.0020	7.238	0.024	2.962	0.013	0.04293	0.00027	0.19350	0.00073	0.4093	0.0016	0.10488	0.00071	0.10486	0.00071
6266-45.7	5.949	0.044	2.393	0.019	1.00e−05	1.00e−05	0.2982	0.0012	7.118	0.024	2.864	0.012	0.04189	0.00016	0.19473	0.00074	0.4023	0.0016	0.10414	0.00046	0.10412	0.00046
6266-46.4	5.956	0.027	2.399	0.013	2.34e−05	2.66e−05	0.3020	0.0021	7.264	0.047	2.925	0.021	0.04158	0.00016	0.19136	0.00077	0.4028	0.0018	0.10324	0.00051	0.10320	0.00051
6266-46.5	5.906	0.031	2.379	0.012	1.30e−06	1.82e−05	0.3011	0.0027	7.179	0.049	2.892	0.019	0.04194	0.00029	0.19228	0.00079	0.4028	0.0014	0.10413	0.00069	0.10413	0.00069
6266-47.3	6.253	0.025	2.527	0.010	1.32e−05	2.68e−05	0.3061	0.0012	7.267	0.024	2.937	0.010	0.04212	0.00014	0.19400	0.00083	0.4042	0.0012	0.10420	0.00037	0.10413	0.00037
6266-48.3	6.014	0.033	2.469	0.012	1.31e−05	3.06e−05	0.3155	0.0013	7.321	0.032	3.006	0.011	0.04310	0.00019	0.19272	0.00116	0.4106	0.0017	0.10496	0.00039	0.10494	0.00040
6266-51.4	6.071	0.025	2.478	0.011	2.73e−05	2.53e−05	0.3036	0.0012	7.298	0.025	2.980	0.011	0.04159	0.00016	0.19581	0.00080	0.4082	0.0015	0.10188	0.00041	0.10182	0.00042
6266-51.5	6.126	0.042	2.474	0.018	1.90e−05	1.00e−05	0.2980	0.0013	7.148	0.025	2.887	0.012	0.04169	0.00015	0.19470	0.00073	0.4038	0.0014	0.10323	0.00042	0.10319	0.00042
6266-51.6	6.151	0.036	2.519	0.013	2.18e−05	3.41e−05	0.3061	0.0022	7.313	0.034	2.995	0.012	0.04185	0.00032	0.19510	0.00154	0.4096	0.0020	0.10218	0.00075	0.10212	0.00075
6266-51.7	6.110	0.038	2.464	0.015	4.52e−05	3.02e−05	0.3004	0.0014	7.176	0.026	2.893	0.011	0.04186	0.00020	0.19483	0.00077	0.4032	0.0015	0.10383	0.00051	0.10373	0.00051
6266-51.8	6.184	0.034	2.504	0.015	1.00e−05	1.00e−05	0.3042	0.0019	7.240	0.038	2.931	0.017	0.04201	0.00018	0.19453	0.00077	0.4049	0.0015	0.10377	0.00053	0.10372	0.00053
6266-52.3	6.003	0.034	2.443	0.010	1.00e−05	1.00e−05	0.3042	0.0022	7.229	0.037	2.941	0.010	0.04209	0.00031	0.19297	0.00115	0.4069	0.0020	0.10343	0.00066	0.10341	0.00066
6266-53.3	5.933	0.024	2.427	0.013	7.94e−06	1.96e−05	0.3103	0.0015	7.296	0.025	2.985	0.014	0.04253	0.00019	0.19303	0.00091	0.4091	0.0018	0.10397	0.00059	0.10396	0.00059
6266-54.4	6.266	0.040	2.563	0.018	6.26e−06	1.65e−05	0.3105	0.0027	7.374	0.048	3.016	0.022	0.04211	0.00026	0.19491	0.00070	0.4090	0.0018	0.10296	0.00071	0.10290	0.00071
6266-54.5	6.262	0.028	2.563	0.011	8.09e−06	2.01e−05	0.3065	0.0014	7.214	0.030	2.953	0.012	0.04248	0.00016	0.19565	0.00079	0.4093	0.0013	0.10378	0.00038	0.10372	0.00038
Average	6.093		2.474		0.000022		0.3041		7.232		2.937		0.0420		0.1942		0.4061		0.1035		0.1035	
Standard deviation	0.122		0.055		0.000018		0.0062		0.067		0.045		0.0006		0.0015		0.0030		0.0011		0.0011	
Standard deviation (%)	2.01		2.24		81.83		2.03		0.92		1.54		1.42		0.76		0.74		1.08		1.08	
Standard error	0.016		0.007		0.0000022		0.00079		0.0085		0.0057		0.00008		0.00019		0.00038		0.00014		0.00014	
Standard error (%)	0.26		0.28		10.39		0.26		0.12		0.20		0.18		0.10		0.09		0.14		0.14	
Skew	−0.08		−0.11		1.84		−0.41		−0.64		−0.52		−0.09		0.26		−0.31		0.05		0.06	
Kurtosis	−0.80		−0.67		4.02		0.23		1.88		0.66		−0.33		0.25		−0.54		0.33		0.28	
Avg. error (%)	0.53		0.58		106.89		0.55		0.45		0.50		0.48		0.47		0.43		0.53		0.53	

content was negligible, with an average $^{204}Pb^+/^{206}Pb^+$ value of 2×10^{-5}, but for completeness the $^{206}Pb^+/^{270}[UO_2]^+$ values were corrected for surface common Pb using ^{204}Pb (Stern, 1997). Although the $^{207}Pb^+$ isotope was not monitored in these particular experiments, HR-SIMS determinations of $^{207}Pb^+/^{206}Pb^+$ in other experiments consistently yield results within error, i.e., Gaussian distributions with MSWD ~ 1. There is no evidence of anomalous $^{207}Pb/^{206}Pb$ in the zircon.

5.3.1. U, Th, Zr isotopes

For experiment IP222.1, the mean $^{254}[UO]^+/^{238}U^+ = 7.225$, $S = 1.2\%$, the average within-spot error $= 0.41\%$, and MSWD $= 9.2$. For IP222.2, the mean $^{254}[UO]^+/^{238}U^+ = 7.232$, $S = 0.92\%$, the average within-spot error $= 0.45\%$, and MSWD $= 6.2$. In both cases, the variations in $^{254}[UO]^+/^{238}U^+$ are small but well outside the within-spot errors. The standard deviation (S) of the $^{254}[UO]^+/^{196}[Zr_2O]^+$ values in IP222.1 and IP222.2 are both 2.0%, and MSWD's are 20 and 16, respectively, suggesting small but measurable variations in uranium concentrations.

The mean $^{248}[ThO]^+/^{254}[UO]^+$ for IP222.1 is 0.1949 (MSWD $= 2.5$; $S = 0.76\%$) and for IP222.2 is 0.1942 (MSWD $= 3.0$; $S = 0.69\%$). The mean $^{248}[ThO]^+/^{254}[UO]^+$ values are 12% less than the accepted Th/U value of 0.221, in contrast with the glass data, which indicated no relative discrimination. There is no significant correlation of $^{254}[UO]^+/^{196}[Zr_2O]^+$ or $^{248}[ThO]^+/^{254}[UO]^+$ with $^{254}[UO]^+/^{238}U^+$. The dispersion of HR-SIMS U and Th abundance measurements and Th/U ratios is identical to the TIMS data, providing evidence that trace element homogeneity is not a function of sample size in this zircon.

5.3.2. U–Pb isotopes

For brevity, the results for IP222.1 are discussed and illustrated, whereas similar results for IP222.2 are only summarized as appropriate. In contrast to the data for SRM 610, the mean $^{206}Pb^+/^{238}U^+$ of 0.3067 (Table 4) is 3.4 × *higher* than the TIMS value. In Fig. 5 are shown the $^{254}[UO]^+/^{238}U^+$ values plotted against $^{206}Pb^+/^{238}U^+$ and $^{206}Pb^+/^{270}[UO_2]^+$. The expected positive correlation in the former case is evident (unweighted linear regression slope for IP222.1 = 0.0624, IP222.2 = 0.0698), in contrast to the lack of an obvious correlation in the case of $^{206}Pb^+/$
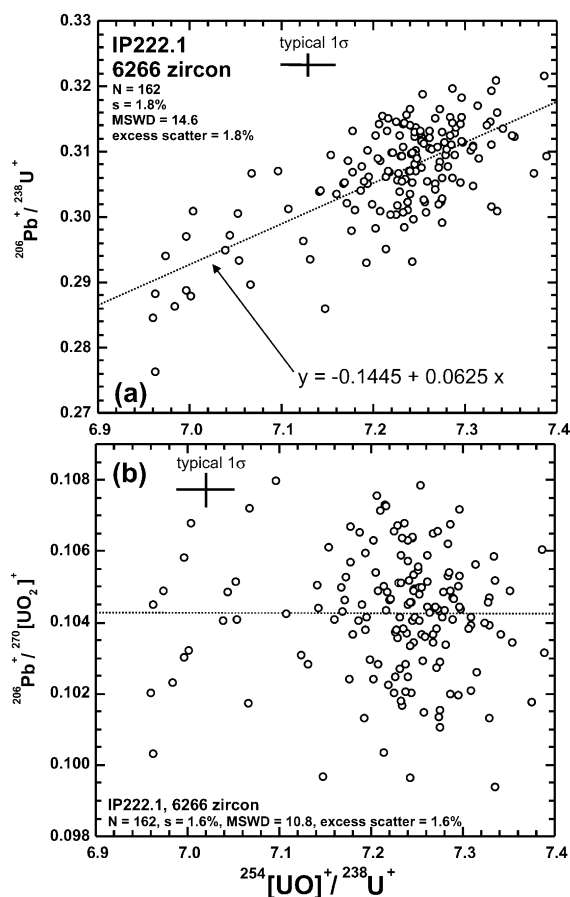
Fig. 5. $^{254}[UO]^+/^{238}U^+$ vs. (a) $^{206}Pb^+/^{238}U^+$ and (b) $^{206}Pb^+/^{270}[UO_2]^+$ for random analyses of z6266 zircon, mount IP222, experiment 1 (IP222.1). Linear least-squares regressions of the dependent variables are plotted (dashed lines); note the absence of significant correlation of the variables in (b). In both cases there is significant excess scatter about the curves.

$^{270}[UO_2]^+$.[1] These results demonstrate that, for the purposes of these experiments, the $^{206}Pb^+/^{270}[UO_2]^+$ values are independent of the concurrent $^{254}[UO]^+/^{238}U^+$ values. Consequently, the process of evaluating the U–Pb isotope discrimination is simplified, e.g., the raw $^{206}Pb^+/^{270}[UO_2]^+$ may be plotted as is, without normalization to a specified $^{254}[UO]^+/^{238}U^+$ value.

---

[1] A linear rather than exponential or power law relationship between $^{254}[UO]^+/^{238}U^+$ and $Pb^+/U[O_x]^+$ is considered adequate to model the distribution of data in a given analytical session of high quality, i.e., in which the spread of $^{254}[UO]^+/^{238}U^+$ is less than ± 0.5 units.

The data set for z6266 obtained for IP222.1 is much larger than, but the results are typical of, the usual 10–20 individual measurements in routine applications.

The mean within-spot error for all $^{206}Pb^+/^{238}U[O_x]^+$ species in IP222.1 (and IP222.2) is $\pm 0.5\%$. The standard deviation of $^{206}Pb^+/^{238}U^+$ lineary projected to the mean $^{254}[UO]^+/^{238}U^+$ (i.e., $\{^{206}Pb^+/^{238}U^+\}_{UO/U}$) is 1.8% (for IP222.2 it is 1.3%), and in the case of the raw $^{206}Pb^+/^{270}[UO_2]^+$ values is 1.6% (IP222.2 = 1.1%). Using the within-spot errors, the calculated excess scatter in $\{^{206}Pb^+/^{238}U^+\}_{UO/U}$ is 1.8%, as indicated by the high MSWD of 14.6 (IP222.2 excess scatter = 1.2%, MSWD = 6.3). For $^{206}Pb^+/^{270}[UO_2]^+$, a slightly lower excess scatter value of 1.6% is calculated, as is the MSWD value of 10.8 (IP222.2 excess scatter = 0.95%, MSWD = 4.5).

Fig. 6(a, dotted curve) shows a probability density distribution for the raw $^{206}Pb^+/^{270}[UO_2]^+$ data for experiment IP222.1. The range of values is 0.0994–0.1080 ($\pm 4.1\%$), considerably greater than the $\pm 0.4\%$ spread in the TIMS data. The distribution is non-Gaussian, displaying one main peak, a secondary 'bump' on the main peak, and tailing to low values. Whether or not real isotopic heterogeneities were encountered, for a data set of this size it is reasonable to expect an approach to the limiting near-Gaussian distribution indicated by the TIMS data (Fig. 3c), albeit with a broader distribution due to the lower precision of each measurement (i.e., $\sim 0.5\%$ vs. 0.08%). The fact that the distribution of $^{206}Pb^+/^{270}[UO_2]^+$ measurements is more complex than that expected from the TIMS data is consistent with the presence of unaccounted instrumental effects. Similar non-Gaussian distributions are exhibited by $\{^{206}Pb^+/^{238}U^+\}_{UO/U}$ and $\{^{206}Pb^+/^{254}[UO]^+\}_{UO/U}$ (i.e., corrected for variable discrimination). For IP222.2, the probability density distribution for $^{206}Pb^+/^{270}[UO_2]^+$ more closely approximates a Gaussian distribution (Fig. 6b), although slight excessive tailing and asymmetry are apparent.

5.3.2.1. Secondary steering corrections to IP222.1. The $^{206}Pb^+/^{238}U[O_x]^+$ measurements for IP222.1 scatter well-beyond that expected if the within-spot errors are sufficient and there are no other sources of variation, such as inhomogeneity in the zircon or unrecognized analytical artifacts. The excess scatter for IP222.1 is 1.6%, whereas for IP222.2 the excess
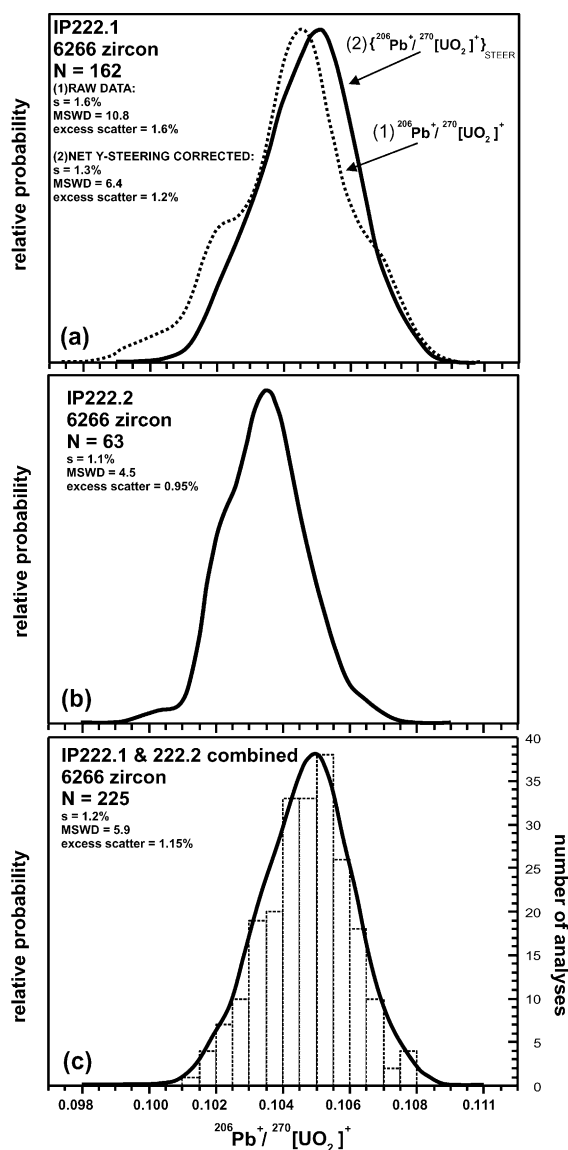
Fig. 6. Probability density distributions of SHRIMP U–Pb data from 61 fragments of z6266 zircon obtained from mount IP222 (see Fig. 2), obtained in two separate experiments (IP222.1, IP222.2). (a) Experiment IP222.1, raw $^{206}Pb^+/^{270}[UO_2]^+$ (dashed line) and the same data corrected for secondary ion steering, $\{^{206}Pb^+/^{270}[UO_2]^+\}_{STEER}$. See text for explanation. (b) Experiment IP222.2 raw $^{206}Pb^+/^{270}[UO_2]^+$. (c) Data from experiments IP222.1 and IP222.2 combined (see text for details), yielding 225 individual analyses of the zircon. Note that the distribution is similar to the limiting distribution defined by the TIMS data (Fig. 3c), but there is excess scatter similar that for SRM 610 (Fig. 4c).

scatter is lower (0.95%). The superior data for IP222.2 were collected from a restricted central region of the bullseye in contrast to IP222.1.

The distribution of mean $^{206}Pb^+/^{270}[UO_2]^+$ values for each grain fragment over the surface of the mount IP222.1 is illustrated in Fig. 7(a). The diagram reveals a tendency to low mean values on the extreme right and high values on the extreme left. These spatially correlated variations in $^{206}Pb^+/^{270}[UO_2]^+$ have not, to our knowledge, been previously described, and provide evidence of spatial control over discrimination. The voltages applied to lenses and deflection plates that control the trajectory of secondary ions within the secondary column are also strongly correlated with the location of the analysis site, particularly for the extreme left and right positions. Fig. 7(b) shows contours of the net y-steering component (see Section 4) across the bullseye for experiment IP222.1. It is apparent that the net y-steering voltage becomes progressively more positive from left to right across the bullseye, with a broad central area of low gradients, and steep gradients towards the perimeter. Fig. 7(c) illustrates a similar effect for the pre-alpha slit z-steering parameter. Although not demonstrated here, the edge effects become progressively stronger across the remaining 0.6 cm of surface to the very edge of the steel holder.

In Fig. 8 are plotted the $^{206}Pb^+/^{270}[UO_2]^+$ values vs. the net y-steering values. A negative linear correlation is evident at net y-steering values greater than -195 V; below this value the data seem unaffected. The correlation, approximated by a quadratic best-fit curve, provides a basis for correcting the $^{206}Pb^+/^{270}[UO_2]^+$ values to a reference net y-steering voltage, i.e.:

$$\{^{206}Pb^+/^{270}[UO_2]^+\}_{STEER} = {}^{206}Pb^+/^{270}[UO_2]^+ \\ *^{206}Pb/^{270}[UO_2]_{ref}/ \\ {}^{206}Pb/^{270}[UO_2]_o$$

where $\{^{206}Pb^+/^{270}[UO_2]^+\}_{STEER}$ is the net y-steering-corrected ratio, $^{206}Pb/^{270}[UO_2]_{ref}$ refers to the calculated value lying on the best-fit curve at the reference net y-steering voltage, and $^{206}Pb/^{270}[UO_2]_o$ is the calculated value on the best-fit curve at the observed net y-steering value. Here, the reference net y-steering voltage was chosen as the mean value (-187 V).
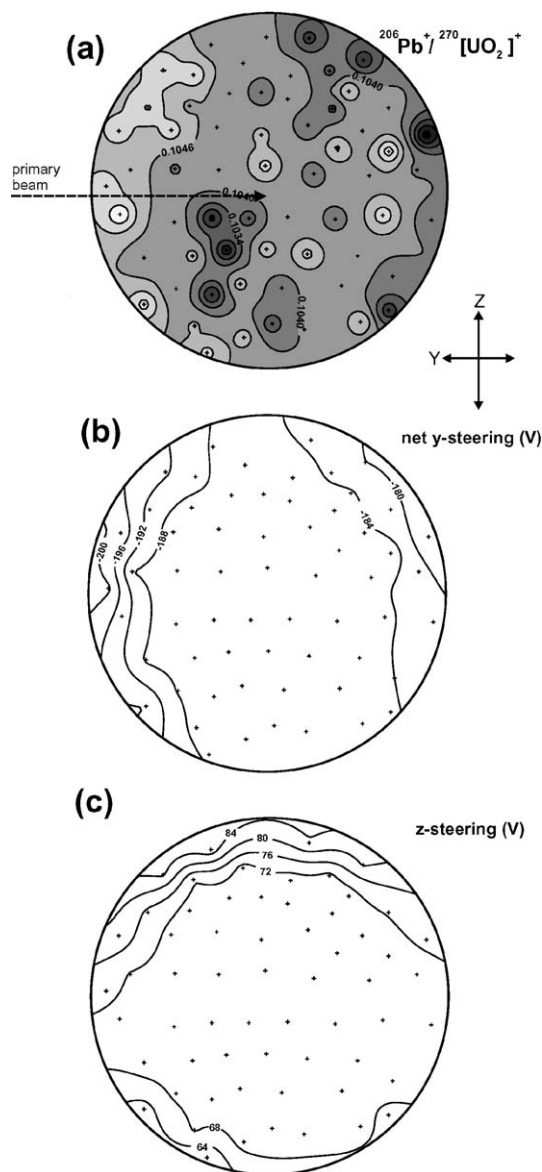
Fig. 7. Contour maps of the 'bullseye' area (Fig. 2) of mount IP222 (experiment 1), illustrating the edge-effects that play a role in causing isotope discrimination. (a) Distribution of mean $^{206}Pb^+/^{270}[UO_2]^+$ values (2–4 measurements per grain). Note the tendency to low mean values on the extreme right and high values on the extreme left of the bullseye. The primary beam impacts the sample at a 45° incidence with the orientation shown, and the sample is moved beneath it to target different grains. Crosses indicate locations of fragments of z6266 zircon. (b) Distribution of net y-steering voltage, a factor reflecting horizontal deflection of secondary ions (see text). (c) Distribution of pre-alpha slit z-steering voltage.
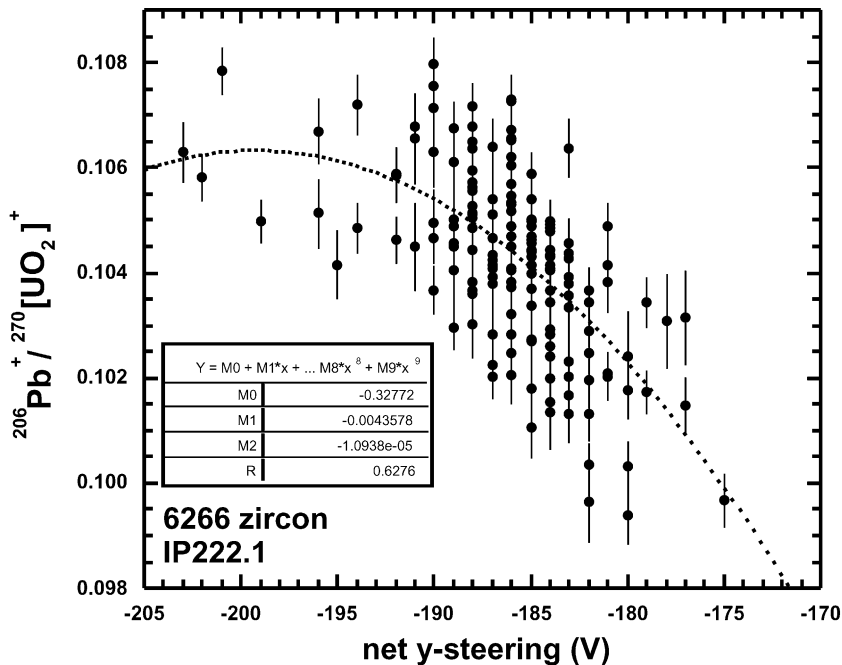
Fig. 8. Mount IP222.1 net y-steering voltage vs. $^{206}Pb^+/^{270}[UO_2]^+$. The diagram illustrates that there is a relationship between secondary ion steering in the y-direction (horizontal) and the measured isotopic ratios, as displayed in Fig. 7. This relationship was used to correct the $^{206}Pb^+/^{270}[UO_2]^+$ values to a reference value of -187 V, and the data are subsequently termed $\{^{206}Pb^+/^{270}[UO_2]^+\}_{STEER}$.

Utilizing only the within-spot errors, the probability density distribution for the $\{^{206}Pb^+/^{270}[UO_2]^+\}_{STEER}$ values is shown in Fig. 6(a, solid curve), which can be compared with the raw data (dotted curve). The range of values is now reduced to $0.1012-0.1077$ ($\pm 3.2\%$), although still considerably greater than the TIMS data, and S is reduced from 1.6% to 1.3%. The MSWD is reduced to 6.4, but an excess scatter of 1.2% per datum remains. There is no systematic correlation of $\{^{206}Pb^+/^{270}[UO_2]^+\}_{STEER}$ with any other instrumental parameters recorded, particulary steering in the z-direction, $^{270}[UO_2]^+$ or $^{196}[Zr_2O]^+$ count rates, or $^{270}[UO_2]^+/^{196}[Zr_2O]^+$.

5.3.2.2. IP222.1 and IP222.2 combined. From accumulated experience measuring $^{206}Pb^+/^{270}[UO_2]^+$ in the z6266 zircon standard it is found that the sessional mean $^{206}Pb^+/^{270}[UO_2]^+$ values differ by typically $\leq 2\%$ when analytical conditions are reproduced as closely as possible. Nevertheless, there are often small differences in technique between sessions that seem to influence the means, and for purpose of combining data sets it is necessary to adjust the data. Accord-

ingly, the $\{^{206}Pb^+/^{270}[UO_2]^+\}_{STEER}$ values for IP222.1 and the $^{206}Pb^+/^{270}[UO_2]^+$ values for IP222.2 (not needing steering correction) were combined to yield a data set of 225 individual analyses, following adjustment of the IP222.2 data. The $^{206}Pb^+/^{270}[UO_2]^+$ values for IP222.2 were multiplied by 1.0123 so that their weighted mean coincided with that of IP222.1 (i.e., 0.1047). The standard deviation for the combined data set is 1.22%, the average error is 0.53%, and the MSWD is 5.9, yielding an excess scatter of 1.15%. The probability density curve (Fig. 6c) indicates a Gaussian distribution with slight negative skew. The range of $^{206}Pb^+/^{270}[UO_2]^+$ values is $0.1012-0.1077$. Again, these calculations include only the within-spot errors, and clearly indicate that these errors alone are insufficient to account for the dispersion of data.

Assuming that the HR-SIMS analyses of z6266 zircon were randomized, it is indisputable that the distribution of $^{206}Pb^+/^{238}U[O_x]^+$ measurements should be equivalent to the limiting distribution determined by TIMS, assuming that the data have been corrected for any spot-to-spot variations in elemental discrim-

ination. Indeed, the probability density plot of all 225 $^{206}Pb^+/^{270}[UO_2]^+$ values is normally distributed, similar to the TIMS data (Figs. 6c and 3c). As such, the mean $^{206}Pb^+/^{270}[UO_2]^+$ value of 0.1047 can be calibrated to the mean TIMS $^{206}Pb/^{238}U$ reference value of 0.090583 (559 Ma). The range of $^{206}Pb^+/^{270}[UO_2]^+$ values is 0.1012–0.1077, from which an apparent age range of 541 ± 8 to 575 ± 5 Ma (2σ, within-spot errors) is calculated.

It could be argued that this age range indicates the presence of fine-scale isotopic heterogeneities, such as areas of Pb-loss or unsupported radiogenic Pb (e.g., Compston, 1999). In such a case, excess scatter in $^{206}Pb^+/^{270}[UO_2]^+$ would be observed due to the orders-of-magnitude smaller masses of material analyzed compared with TIMS, thus enhancing the chances of analyzing extreme age end-members. As such, it could be proposed that the highest and lowest measured $^{206}Pb^+/^{270}[UO_2]^+$ values for the zircon have sampled such heterogeneities. If the apparent $^{206}Pb/^{238}U$ ages did in fact vary on a microscale due to recent Pb-loss, they could not exceed the TIMS $^{207}Pb^*/^{206}Pb^*$ age of 562.6 ± 0.4 Ma, however, the maximum apparent HR-SIMS $^{206}Pb/^{238}U$ age of 575 Ma is well in excess. Clearly, if age heterogeneities were present, they cannot relate to recent Pb-loss. In order for the scatter in apparent ages to be real, the zircon would have to contain micron-scale isotopic heterogeneities with components at least as distinct as 541 and 575 Ma. But the TIMS and HR-SIMS data sets suggest that only one age component exists.

6. Discussion

In Section 4.1, we defined three levels of increasing uncertainty related to individual HR-SIMS U–Pb analyses, namely, the within-spot, within-session, and external errors (Fig. 1). The $^{208}Pb^+/^{206}Pb^+$ data for SRM 610 glass demonstrate that the method of estimating within-spot errors is valid, i.e., sufficient to explain the observed variability in multiple spot measurements of this isotopically homogeneous target. A similar evaluation of within-spot errors could have been accomplished by repeat isotopic analyses from the same spot location.

On the other hand, the raw $^{248}[ThO]^+/^{254}[UO]^+$ measurements of multiple spots on SRM 610 glass did

not agree according to the within-spot errors. In this case, however, correction of the raw ratios for a slight but systematic pattern of variable discrimination yielded results that were also adequately explained solely by the within-spot errors, i.e., there was no requirement to propagate additional errors related to the corrections for variable discrimination. Homogeneity in Th/U for the glass is clearly supported, consistent with results from previous studies (Hinton et al., 1995; Rocholl et al., 2000). The $^{248}[ThO]^+/^{254}[UO]^+$ results demonstrate that, for a homogeneous sample, the within-spot errors should be quite adequate to explain the dispersion between spot elemental analyses that have been suitably corrected for any variability in discrimination, i.e., the within-session errors = within-spot errors.

Nevertheless, this prediction was not held in the case of the Pb/U ratios in SRM 610 glass and z6266 zircon. The TIMS data for SRM 610 do not support the possibility that Pb/U is necessarily more heterogeneous than Th/U. For the glass, the observed excess scatter of 0.95% in $^{206}Pb^+/^{270}[UO_2]^+$ and the non-Gaussian distribution of data (Fig. 4c) suggest the presence of unaccounted analytical artifacts. The excess scatter for SRM 610 cannot be explained by matrix differences between spots, or differences in secondary ion steering between spots, as in both cases there were none. The combined $^{206}Pb^+/^{270}[UO_2]^+$ data set for z6266 zircon also indicates the presence of significant dispersion of the data beyond the calculated within-spot analytical errors, with a calculated excess scatter of 1.15% (Fig. 6c). That the degree of excess scatter is similar to that determined for SRM 610 suggests that the zircon cannot be significantly more heterogeneous in Pb/U. Taken together, both the zircon and glass HR-SIMS data sets strongly indicate the existence of residual variability in the discrimination between Pb^+ and the $U[O_x]^+$ species. Without resorting to sample heterogeneity as an explanation, we must conclude that U and Pb ions were more strongly affected by subtle differences in analytical conditions compared with, for example, Th/U.

Attempts to determine patterns for, and remove, the unexplained dispersion in $^{206}Pb^+/^{238}U[O_x]^+$ were unsuccessful in this study. Such results are also typical of the smaller data sets accumulated in routine U–Pb analytical sessions. Consequently, if $^{206}Pb^+/^{238}U[O_x]^+$ data within a particular session are to be compared,

we must not make the mistake of assuming the within-session errors are equivalent to the $\pm 0.5\%$ within-spot errors. This brings us to the question of what is a valid lower limit of the within-session errors. The minimum within-session error is the standard deviation (S) of the variable-discrimination-corrected $^{206}Pb^+/^{238}U[O_x]^+$ values or U–Pb calibration constants calculated for the standard (S_{ref}; see Fig. 1). The method of estimating the relative discrimination (if any) between spots matters only to the extent it actually works in reducing S_{ref}.

For reference materials with low U and Pb, the within-spot errors may expand and eliminate any excess error. In such cases, however, it is important to recognize that a minimum within-session error still exists for all data in the session, and it is S_{ref}. Unknown data having within-spot errors lower than S_{ref} should be set to the latter (Fig. 1). Estimating S_{ref} within each analytical session is the preferred method because it integrates all the potential instrumental problems. It is important to note, however, that most labs use fragments of in-house zircon standards located within each unknown mount, and that determining S_{ref} may be influenced by sample heterogeneity, which may cause S_{ref} to seem unrealistically high. In other cases, 'outlier' rejection based on the assumption of reference material heterogeneity my cause S_{ref} to appear unrealistically low. In either case, particularly the latter, a lower bound on S_{ref} (e.g., 1%) should be adopted, as determined from specialized experiments with SRM 610 or other reliable reference material. Note that it is *not* necessary to utilize a zircon standard to estimate S_{ref}.

In determining the additional uncertainty to be propagated to the external error in the spot $^{206}Pb/^{238}U$ age, the issue here is the uncertainty in the absolute discrimination correction (Fig. 1). We are concerned here with the uncertainty introduced in the value of the mean of the discrimination-corrected $^{206}Pb^+/^{238}U[O_x]^+$ values or U–Pb calibration constants for the reference material, which is simply the standard error of such data (SE_{ref}). If a weighted mean and error calculation is preferred in determining the uncertainty (i.e., σ_{ref}), it is required to use the within-session errors, not the potentially underestimated within-spot errors. Other sources of error are presumed to be insignificant, including matrix differences between standard and unknown, common Pb and deadtime corrections, and the absolute (TIMS) $^{206}Pb/^{238}U$ age of the zircon actually utilized. Concerning the latter, there needs to be an adequate number of HR-SIMS analyses of the standard to rule out systematic errors due to insufficient sampling if real age heterogeneities are expected (cf., Compston, 2000). Where there exist sufficient data upon the homogeneous standard, SE_{ref} or σ_{ref} can in most cases be reduced to insignificance relative to the within-session errors.

7. Conclusions

In this study, we have distinguished three types of error estimates for individual ion microprobe zircon $^{206}Pb/^{238}U$ zircon analyses: within-spot, within-session (internal), and external errors (Fig. 1). SHRIMP II ion microprobe experiments conducted upon SRM 610 glass have demonstrated that the methods described here of estimating within-spot analytical errors of isotopic (e.g., $^{208}Pb^+/^{206}Pb^+$) and elemental (e.g., $^{248}[ThO]^+/^{254}[UO]^+$) ratios are reasonably accurate. The within-spot errors are based upon counting statistics for the individual isotopes augmented by any additional scatter encountered during the analysis. By whatever scheme the within-spot errors are calculated, the simple experiment of obtaining MSWD's near unity for repeat analyses of a homogeneous sample is crucial in demonstrating that these errors are not too large or small.

The SRM 610 experiments also show that, for a target that is chemically homogeneous, ~ 15-μm scale spot-to-spot reproducibility in elemental ratios is expected using the within-spot analytical errors, after corrections (e.g., using $^{254}[UO]^+/^{238}U^+$) for any systematic spot-to-spot elemental discrimination. That is, no additional uncertainty was introduced when going from spot-to-spot. TIMS $^{206}Pb/^{238}U$ and ion microprobe trace element data on SRM 610 from this study and others provide every reason to expect the Pb/U ratios to behave similarly, yet it was not possible to reproduce the $^{206}Pb^+/^{238}U[O_x]^+$ ratios, appropriately corrected for systematic discrimination, from spot-to-spot using the within-spot errors of about $\pm 0.5\%$.

A similar conclusion was drawn from SHRIMP experiments upon a gem zircon reference material (z6266). Here, TIMS $^{206}Pb/^{238}U$ data for fragments

of the zircon indicated isotopic homogeneity (559.0 ±
0.2 Ma) on the bulk scale. Despite correcting the
SHRIMP data for z6266 zircon for well-known and
other lesser-known analytical artifacts causing varia-
ble discrimination of Pb and U ions, it was also not
possible to reproduce the $^{206}Pb^+/^{238}U[O_x]^+$ ratios from
spot-to-spot to the within-spot analytical errors of
about ± 0.5%.

In both SRM 610 glass and z6266 zircon there
remained a similar level of data ('excess') scatter
beyond that expected from the within-spot errors,
about ± 1% (1σ) per $^{206}Pb^+/^{238}U[O_x]^+$ analysis. It is
concluded that the methods of correcting for discrim-
ination of Pb and U ions while analyzing zircon, such as
normalization to $^{254}[UO]^+/^{238}U^+$, were not sufficient to
remove all analytical artifacts. It is argued that the
within-session errors for $^{206}Pb/^{238}U$ cannot be smaller
than the standard deviation of the discrimination-cor-
rected $^{206}Pb^+/^{238}U[O_x]^+$ or the calibration constant(s)
for the reference material (S_{ref}). The value of S_{ref} may
be determined for each analytical session if reliable
standards are analyzed, or in separate specialized
experiments utilizing SRM 610 or other homogenous
standards. For the external errors there exists an addi-
tional error component quantified by the standard
deviation of the mean of the discrimination-corrected
$^{206}Pb^+/^{238}U[O_x]^+$ or for the calibration constant(s) for
the zircon reference material (SE_{ref} or σ_{ref}); this error
may be small enough to be ignored if the reference
material is reliable and sufficient data are collected.

Although these conclusions were developed for
$^{206}Pb/^{238}U$ in zircon, they are equally applicable to
any isotopic ratio in any mineral. The conclusions rest
on the assumption that the reference materials utilized
are homogeneous at the scale sampled by the ion
microprobe. The problem is that the degree of homo-
geneity of U/Pb in a given standard at the equivalent
scale sampled by the ion microprobe cannot presently
be determined with a completely independent techni-
que. Although it is true that the orders-of-magnitude
smaller masses of material analyzed by HR-SIMS
improve the chances of discovering U–Pb isotopic
heterogeneities, we consider it a case of special
pleading if somehow such heterogeneities are argued
to occur in the best-available reference materials at a
scale that only HR-SIMS seems capable of detecting.
Furthermore, there *are* well-recognized patterns of
U–Pb isotope discrimination in HR-SIMS analysis

of zircon, for example correlations with $^{254}[UO]^+/$
$^{238}U^+$, but these relationships are entirely empirical
and must be viewed as first approximations of a
complex array of factors causing discrimination. A
previously unknown or little-discussed factor causing
discrimination that is related to the position of sam-
ples on the mount was identified in this study, and
there is little doubt that other instrumental factors
exist. The ions of Pb and U seem to be more strongly
affected by subtle and as yet unknown differences in
experimental conditions that exist between spot anal-
yses compared with ions of U and Th. For SRM 610,
it is noteworthy that where there was no significant
relative elemental discrimination, as in the case of
$^{248}[ThO]^+/^{254}[UO]^+$, no excess errors were found;
where discrimination was evident, as in the case of
$^{206}Pb^+/^{238}U[O_x]^+$, excess scatter resulted. We do not
believe that this relationship is best explained by
invoking sample heterogeneity.

It should be mentioned that, unfortunately, it is not
possible to eliminate the need to go from spot-to-spot in
replicating the $^{206}Pb^+/^{238}U[O_x]^+$ values in zircon or
glass. The $^{206}Pb^+/^{238}U[O_x]^+$ values change systemati-
cally with sputter duration, or more precisely the extent
of oxygen implantation in the zircon, and so it is not
possible to simply take replicate measurements from
the same spot, as can be done with $^{208}Pb^+/^{206}Pb^+$ or
$^{248}[ThO]^+/^{254}[UO]^+$. Sputter duration must be equiv-
alent between spots, and is one of a number of potential
causes of unaccounted variation between spots.

The reference materials used in this study effec-
tively rule out structurally or compositionally related
matrix effects as other potential sources of error. The
excess scatter could result from either uncontrolled
variations in secondary ion extraction and transmis-
sion, or perhaps to vagaries of the ion detection
system, such as sensitivity to beam position on the
first dynode of the electron multiplier. Whatever the
cause, a significant reduction in the analytical errors
resulting from HR-SIMS U–Pb analysis of zircon can
only be made if the sensitivity of U and Pb ions to
analytical conditions can be reduced or modelled.

It was shown that there are some advantages in
utilizing $^{270}[UO_2]^+$ rather than $^{238}U^+$ or $^{254}[UO]^+$ in
the determination of $^{206}Pb/^{238}U$ ages of zircon. The
main benefit is that the $^{206}Pb^+/^{270}[UO_2]^+$ values are
practically independent of the concurrently measured
$^{254}[UO]^+/^{238}U^+$ values, and so the usual concerns

about variable, $^{254}[UO]^+/^{238}U^+$-correlated discrimination from spot-to-spot are virtually eliminated. Accordingly, it is not essential to collect data for $^{254}[UO]^+$ or $^{238}U^+$, thus reducing by one the number of isotopes required for a zircon analysis. Counting statistics are also most favourable with $^{270}[UO_2]^+$.

Nevertheless, the current methods are all very similar in their approach, that is, correction of measured $^{206}Pb^+/^{238}U[O_x]^+$ for discrimination by comparison with a standard, and all likely suffer from the same sensitivity of discrimination to analytical conditions. In the absence of a suitable zircon standard, the use of SRM 610 should prove useful in carrying out periodic evaluations of instrument performance and ability to reproduce $^{206}Pb^+/^{238}U[O_x]^+$ ratios. The use of a natural zircon standard remains essential for routine work because the discrimination of Pb and U ions in SRM 610 glass relative to the accepted values is not the same sense or magnitude as for zircon.

Acknowledgements

References

Amelin, Y.A., 1998. Geochronology of the Jack Hills detrital zircons by precise U–Pb isotope dilution analysis of crystal fragments. Chem. Geol. 146, 25–38.

Amelin, Y.A., Heaman, L.M., Verchogliad, V.M., Skobelev, V.M., 1994. Geochronological constraints on the emplacement of an anorthosite–rapikivi granite suite: U–Pb zircon and baddeleyite study of the Korosten complex, Ukraine. Contrib. Mineral. Petrol. 116, 411–419.

Claoué-Long, J.C., Compston, W., Roberts, J., Fanning, C.M., 1995. Two Carboniferous ages: a comparison of SHRIMP zircon dating with conventional zircon ages and $^{40}Ar/^{39}Ar$ analysis. In: Berggren, W.A., Kent, D.V., Aubry, M.-P., Hardenbol, J. (Eds.), (Eds.), Geochronology, Time Scales and Global Strati-

graphic Correlation. SEPM Special Publication. Society for Sedimentary Geology, Tulsa, USA, pp. 3–21.

Compston, W., 1999. Geological age by instrumental analysis: the 29th Hallimond Lecture. Mineral. Mag. 63, 297–311.

Compston, W., 2000. Interpretations of SHRIMP and isotope dilution zircon ages for the geological time-scale: I. The early Ordovician and late Cambrian. Mineral. Mag. 64, 43–57.

Compston, W., Williams, I.S., Meyer, C., 1984. U–Pb geochronology of zircons from lunar breccia 73217 using a sensitive high mass-resolution ion microprobe. J. Geophys. Res. 89, B525–B534.

Hinthorne, J.R., Andersen, C.A., Conrad, R.L., Lovering, J.F., 1979. Single-grain $^{207}Pb/^{206}Pb$ and U/Pb age determinations with a 10 micron spatial resolution using the ion microprobe mass analyzer. Chem. Geol. 25, 271–303.

Hinton, R.W., Harte, B., Witt-Eickschen, G., 1995. Ion probe measurements of National Institute of Standards and Technology Standard Reference Material SRM 610 glass, trace elements. Analyst 120, 1315–1319.

Holliger, P., 1992. SIMS isotope analysis of U and Pb in uranium oxides: geological and nuclear applications. In: Benninghoven, A., Janssen, K.T.F., Tümpner, J., Werner, H.W. (Eds.), (Eds.), Eighth International Conference on Secondary Ion Mass Spectrometry (SIMS VIII). Wiley, Chichester, UK, pp. 719–722.

Kane, J.S., 2001. The use of reference materials: a tutorial. Geostand. Newsl. 25, 7–22.

Krogh, T.E., 1973. A low contamination method for hydrothermal decomposition of zircon and extraction of U and Pb for isotopic age determinations. Geochim. Cosmochim. Acta 37, 485–494.

Ludwig, K.R., 2001a. SQUID 1.02: A User's Manual. Special Publication, vol. 2. Berkeley Geochronology Center, Berkeley.

Ludwig, K.R., 2001b. User's Manual for Isoplot/Ex Rev. 2.49: A Geochronological Toolkit for Microsoft Excel. Special Publication, vol. 1a. Berkeley Geochronology Center, Berkeley.

Mendenhall, W., Sincich, T., 1995. Statistics for Engineering and the Sciences, Prentice-Hall, Englewood Cliffs, NJ.

Parrish, R.R., Roddick, J.C., Loveridge, W.D., Sullivan, R.W., 1987. Uranium–lead analytical techniques at the geochronology laboratory, Geological Survey of Canada, Current Research. Radiogenic Age and Isotopic Studies: Report 1. Geological Survey of Canada, Ottawa, Canada, pp. 3–7.

Pearce, N.J.G., et al., 1997. A compilation of new and published major and trace element data for NIST SRM 610 and NIST SRM 612 glass reference materials. Geostand. Newsl. 21, 115–144.

Reed, W.P., 1992. Certificate of Analysis: Standard Reference Materials 610 and 611. National Institute of Standards and Technology.

Rocholl, A.B.E., et al., 1997. Chemical characterization of NIST silicate glass certified reference material SRM 610 by ICP-MS, TIMS, LIMS, SSMS, INAA, AAS, and PIXE. Geostand. Newsl.: J. Geostand. Geoanalysis 21, 101–114.

Rocholl, A., Dulski, P., Raczek, I., 2000. New ID-TIMS, ICP-MS and SIMS data on the trace element composition and homogeneity of NIST Certified Reference Material SRM 610–611. Geostand. Newsl.: J. Geostand. Geoanalysis 24, 261–274.

Roddick, J.C., van Breemen, O., 1994. U–Pb zircon dating: a comparison of ion microprobe and single grain conventional

analyses, current research. Radiogenic Age and Isotopic Studies: Report 8. Geological Survey of Canada, Ottawa, Canada, pp. 1–9.

Silverman, B.W., 1986. Density Estimation for Statistics and Data Analysis. Chapman & Hall, London. 175 pp.

Stacey, J.S., Kramers, J.D., 1975. Approximation of terrestrial lead isotope evolution by a two-stage model. Earth Planet. Sci. Lett. 26, 207–221.

Steiger, R.H., Jäger, E., 1977. Subcommision on geochronology: convention on the use of decay constants in geo- and cosmochronology. Earth Planet. Sci. Lett. 36, 359–362.

Stern, R.A., 1997. The GSC Sensitive High Resolution Ion Microprobe (SHRIMP): analytical techniques of zircon U–Th–Pb age determinations and performance evaluation, current research. Radiogenic Age and Isotopic Studies: Report 10. Geological Survey of Canada, Ottawa, Canada, pp. 1–31.

Stern, R.A., 2000. The significance of secondary ion energy profiles for understanding inter-element calibration curve in SIMS analysis of zircon and monazite. Beyond 2000: New Frontiers in Isotope Geoscience. Abstracts and Proceedings. The University of Melbourne, Lorne, Australia, pp. 167–170.

Stern, R.A., 2001. A new isotopic and trace element standard for the ion microprobe: preliminary TIMS U–Pb and electron microprobe data, current research. Radiogenic Age and Isotopic Studies: Report 14. Geological Survey of Canada, Ottawa, Canada.

Whitehouse, M.J., Claesson, S., Sunde, T., Vestin, J., 1997. Ion microprobe U–Pb zircon geochronology and correlation of Archaean gneisses from the Lewisian Complex of Gruinard Bay, northwestern Scotland. Geochim. Cosmochim. Acta 61, 4429–4438.

Williams, I.S., 1998. U–Th–Pb geochronology by ion microprobe. In: McKibben, M.A., Shanks, I., Ridley, W.C.P., Ridley, W.I. (Eds.), (Eds.), Applications of Microanalytical Techniques to Understanding Mineralizing Processes. Reviews in Economic Geology. Society of Economic Geologists, Socorro, USA, pp. 1–35.

Wittmaack, K., 1979. Secondary ion mass spectrometry as a means of surface analysis. Surf. Sci. 89, 668–700.

Woodhead, J.D., Hergt, J.M., 2001. Strontium, neodymium and lead isotope analyses of NIST glass certified reference materials: SRM 610, 612, 614. Geostand. Newsl.: J. Geostand. Geoanalysis 25 (2–3), 261–266.

York, D., 1969. Least squares fitting of a straight line with correlated errors. Earth Planet. Sci. Lett. 5, 320–324.